



---

*Research Article: New Research | Disorders of the Nervous System*

## Hypoxia Inducible Factor 1 alpha (HIF-1 $\alpha$ ) counteracts the acute death of cells transplanted into the injured spinal cord

<https://doi.org/10.1523/ENEURO.0092-19.2019>

**Cite as:** eNeuro 2019; 10.1523/ENEURO.0092-19.2019

Received: 12 March 2019

Revised: 10 August 2019

Accepted: 19 August 2019

---

This Early Release article has been peer-reviewed and accepted, but has not been through the composition and copyediting processes. The final version may differ slightly in style or formatting and will contain links to any extended data.

**Alerts:** Sign up at [www.eneuro.org/alerts](http://www.eneuro.org/alerts) to receive customized email alerts when the fully formatted version of this article is published.

Copyright © 2019 David et al.

This is an open-access article distributed under the terms of the Creative Commons Attribution 4.0 International license, which permits unrestricted use, distribution and reproduction in any medium provided that the original work is properly attributed.

**1. Manuscript Title:** Hypoxia Inducible Factor 1 alpha (HIF-1 $\alpha$ ) counteracts the acute death of cells transplanted into the injured spinal cord.

**2. Abbreviated Title:** VP16-HIF1 $\alpha$  and SC Transplantation for SCI

**3. Authors:** Brian T. David<sup>1,2</sup>, Jessica J. Curtin<sup>1,2</sup>, David C. Goldberg<sup>1,2</sup>, Kerri Scorpio<sup>1,2</sup>, Veena Kandaswamy<sup>1,2</sup>, and Caitlin E. Hill<sup>1,2</sup>

**Affiliations:**

<sup>1</sup> Burke Neurological Institute, White Plains, NY, United States

<sup>2</sup> Weill Cornell Medicine, Feil Family Brain and Mind Research Institute, New York, NY, United States

**ORCID ID:**

Caitlin Elizabeth Hill: 0000-0002-7356-2843

Brian T. David: 0000-0001-8470-802X

Jessica J. Curtin: 0000-0002-3529-2168

David Goldberg: 0000-0002-9622-4708

Kerri Scorpio: 0000-0002-1161-2809

Veena Kandaswamy: 0000-0001-5517-3599

**4. Author Contributions:** CEH Designed the research, CEH, BD, JC, DG, KS and VK Performed the research; CEH and BD Analyzed the data and Wrote the paper.

**5. Correspondence should be addressed to:**

Caitlin E. Hill

Neural Stem Cell Institute

1 Discovery Way

Rensselaer, NY 12144

caitlinhill@neuralsci.org

Brian T. David

Rush University Medical Center

1725 W. Harrison St., Suite 855

Chicago, IL 60612

Brian\_David@rush.edu

**6. Number of Figures:** 4

**7. Number of Tables:** 1

**8. Number of Multimedia:** 0

**9. Number of words for Abstract:** 248

**10. Number of words for Significance Statement:** 117

**11. Number of words for Introduction:** 921

**12. Number of words for Discussion:** 2949

**13. Acknowledgements:** The authors would like to thank Dr. Rajiv Ratan and the members of the Ratan lab, in particular Dr. Saravanan Karuppagounder, for assistance and advice with western blotting and IVIS experiments as well as providing the reagents (viruses and plasmids) that got this project started. The authors would also like to thank Elena Cheperko, and Abhay Deskmukh for assistance with surgeries and/or animal

care; Danika Brodak for initial Schwann cell isolation and Jennifer Brown for *in vitro* assay optimization.

**14. Conflict of Interest:** The authors declare no competing financial interests.

**15. Funding sources:** This work was supported by the Burke Foundation, White Plains, NY; NIH: NINDS (Grant: NS075375) and the New York State Spinal Cord Injury Research Program: equipment grants (C030081, C029128).

77 **ABSTRACT**

78 Cellular transplantation is in clinical testing for a number of central nervous system  
79 disorders, including spinal cord injury (SCI). One challenge is acute transplanted cell  
80 death. To prevent this death, there is a need to both establish when the death occurs  
81 and develop approaches to mitigate its effects. Here, using luciferase (luc) and green  
82 fluorescent protein (GFP) expressing Schwann cell (SC) transplants in the contused  
83 thoracic rat spinal cord 7 days post-injury, we establish via *in vivo* bioluminescent (IVIS)  
84 imaging and stereology that cell death occurs prior to 2-3 days post-implantation. We  
85 then test an alternative approach to the current paradigm of enhancing transplant  
86 survival by including multiple factors along with the cells. To stimulate multiple cellular  
87 adaptive pathways concurrently, we activate the hypoxia inducible factor 1 alpha (HIF-  
88 1 $\alpha$ ) transcriptional pathway. Retroviral expression of VP16-HIF-1 $\alpha$  in SCs increased  
89 HIF- $\alpha$  by 5.9-fold and its target genes implicated in oxygen transport and delivery  
90 (VEGF, 2.2-fold) and cellular metabolism (enolase, 1.7-fold). In cell death assays *in*  
91 *vitro*, HIF-1 $\alpha$  protected cells from H<sub>2</sub>O<sub>2</sub>-induced oxidative damage. It also provided  
92 some protection against camptothecin-induced DNA damage, but not thapsigargin-  
93 induced endoplasmic reticulum stress or tunicamycin-induced unfolded protein  
94 response. Following transplantation, VP16-HIF-1 $\alpha$  increased SC survival by 34.3%. The  
95 increase in cell survival was detectable by stereology, but not by *in vivo* luciferase or  
96 *in vivo* GFP IVIS imaging. The results support the hypothesis that activating adaptive  
97 cellular pathways enhances transplant survival and identifies an alternative pro-survival  
98 approach that, with optimization, could be amenable to clinical translation.

99

100 **SIGNIFICANCE STATEMENT**

101 To maximize the benefits of cellular transplants for human therapeutic use, there is a  
102 critical need to develop strategies that effectively promote transplant survival and permit  
103 rapid assessment of transplant survival. The current study: 1) identifies the narrow time  
104 window in which transplanted cells die within the injured rat spinal cord, thus  
105 establishing the time window in which cytoprotection should be targeted to counteract  
106 transplanted cell death; 2) tests the effects of elevating HIF-1 $\alpha$  on spinal cord transplant  
107 survival, thus demonstrating that activating adaptive transcriptional pathways is  
108 protective in SCI, and; 3) demonstrates, by comparing three approaches to quantifying  
109 transplant survival, that until faster and more sensitive methods can be developed,  
110 stereology remains the most reliable method.

111

## 112 1. INTRODUCTION

113 The death of transplanted cells is a common feature of cell transplants. In the central  
114 nervous system, the majority of cells die soon after transplantation (Emgard et al., 2003;  
115 Bakshi et al., 2005; Hill et al., 2006; Hill et al., 2007). This undesirable consequence of  
116 transplantation, separate from immune-mediated rejection, poses a challenge to the  
117 therapeutic use of cellular transplants for neurological repair. Development of  
118 approaches that counteract transplanted death are needed to mitigate the deleterious  
119 effects of the acute cell death and maximize the clinical utility of cell transplantation.

120 A necessary first step in developing interventions to counteract transplanted cell  
121 death is to accurately establish when post-transplantation (post-TP) the death occurs. In  
122 experimental models of spinal cord injury (SCI), 1-35% of cells remain after one week  
123 (Barakat et al., 2005; Karimi-Abdolrezaee et al., 2006; Hill et al., 2007), indicating that  
124 most transplant death occurs in the first week post-TP. Based on assessments of cell  
125 death markers, transplanted cell death peaks within 24 h (Hill et al., 2007). However,  
126 the exact time window of transplanted cell death remains to be established. This is due,  
127 in part, to the time-consuming nature of histological quantification of transplanted cells  
128 and the fact that few methods currently exist to rapidly screen transplanted cell survival.  
129 Establishment of the time frame in which transplanted cells die is necessary to  
130 temporally target cell survival interventions. *In vivo* imaging of luminescence can detect  
131 expression of reporters (Ratan et al., 2008), antibodies (Aminova et al., 2008), and  
132 transplanted cells (Okada et al., 2005; Chen et al., 2006; Kim et al., 2006; Roet et al.,  
133 2012), including a reduction in cells over time (Okada et al., 2005; Roet et al., 2012). In  
134 the current study, we use *in vivo* bioluminescence imaging to establish the time window  
135 of transplanted cell death following engraftment into the injured rat spinal cord. We also

136 test the efficacy of both *in vivo* luminescence imaging and *ex vivo* fluorescence imaging  
137 as alternatives to the use of stereology for assessment of transplant survival.

138 To counteract the potentially deleterious effects of acute transplanted cell death,  
139 interventions that promote transplant survival and are amenable to clinical translation  
140 are needed. Historically, transplant survival approaches have focused on targeting  
141 single factors (Nakao et al., 1994; Mundt-Petersen et al., 2000; Karlsson et al., 2002;  
142 Hill et al., 2010). To date, the presence of multiple potential cell death inducers (e.g.,  
143 hypoxia, oxidative stress, excitotoxicity, lack of substrate/adhesion/growth factors) and  
144 the complex cross-talk between cell death pathways has limited the efficacy of this  
145 approach. An alternative approach that has proven efficacious, and which does not  
146 require identifying the factors responsible for the acute cell death, is the activation of  
147 survival pathways. In the injured spinal cord, inclusion of growth factors (Lu et al., 2012;  
148 Robinson and Lu, 2017) or enhancement of growth factor signaling (Golden et al., 2007)  
149 is effective. In other cell transplantation models, mildly stressing the cells to pre-  
150 condition them prior to engraftment is effective (Murry et al., 1986; Theus et al., 2008;  
151 Yu et al., 2013). Although beneficial in preclinical models, implementation as part of a  
152 clinical-grade product may prove challenging. Both growth factor signaling and  
153 preconditioning activate pro-survival transcriptional programs. Directly engaging  
154 transcription factors could provide an alternative means to engage survival pathways.

155 Among the transcription factors implicated in adaptive responses to cellular stress  
156 are members of the hypoxia inducible factor (HIF) family. The HIFs are DNA-binding  
157 transcription factors that consist of an oxygen-labile  $\alpha$ -subunit and a constitutively  
158 expressed  $\beta$ -subunit. By altering the cell's metabolic program and gene expression,  
159 HIF- $\alpha$  signaling allows cells to sense and adapt to environmental stressors such as

160 decreased oxygen and nutrients. HIFs regulate the expression of genes involved in  
161 adaptive transcriptional responses to improve cell survival by enhancing intracellular  
162 ATP and oxygen levels and decreasing the production of reactive oxygen species  
163 (ROS) in times of hypoxic stress (Semenza, 2007). The genes regulated by HIF- $\alpha$   
164 include key pathways needed for cell survival, such as: glucose metabolism/ATP  
165 production, oxygen transport and delivery, and cell growth and fate (Schodel et al.,  
166 2013). The diversity of genes regulated by HIF- $\alpha$  shows that its protective effects are  
167 not limited to hypoxic environments. In a variety of injury models, elevation of HIF-1 $\alpha$  in  
168 transplanted cells enhances transplanted cell survival (e.g., Theus et al., 2008; Wu et  
169 al., 2010). Moreover, pharmacological manipulators of HIFs exist, which makes clinical  
170 targeting of this pathway viable.

171 In this study, in order to examine the effects of HIF-1 $\alpha$  on transplant survival,  
172 Schwann cells (SCs) were used. In preclinical SCI models, extensive examination has  
173 established that they promote axonal growth and remyelinate axons. A comprehensive  
174 review of SC preclinical studies exists, comparing their effects with other cellular  
175 therapies (Tetzlaff et al., 2010). Furthermore, a completed Phase 1 clinical trial  
176 established their safety in humans with SCI (Anderson et al., 2017).

177 The current study establishes the time window post-TP in which cells die following  
178 engraftment into the sub-acutely injured spinal cord. It tests the hypothesis that  
179 transplanted cells die early after implantation due to inadequate activation of  
180 transcription factor pathways necessary for cells to adapt to stress and survive. Using  
181 viral expression of a non-hydroxylatable version of HIF-1 $\alpha$ , the effect of HIF-1 $\alpha$  on  
182 cytoprotection is assessed *in vitro* and *in vivo* following transplantation into the injured  
183 spinal cord. In an effort to identify methods to facilitate the screening of transplant



184 survival, this study also compares three different techniques for assessment of  
185 transplant survival in rats: histological quantification, *ex vivo* fluorescent imaging of  
186 transplanted spinal cords, and *in vivo* bioluminescent imaging.

187

## 188 **2. MATERIALS AND METHODS**

### 189 **2.1 Generation of SCs:**

190 SCs were isolated from the sciatic nerves of adult female Fischer 344 rats (11-12  
191 weeks of age; Harlan barrier 217; www.envigo.com) following published protocols  
192 (Morrissey et al., 1991). The following modification was made: instead of initially  
193 growing the nerves in D-10 [DMEM (Thermo Fisher Scientific) with 10% heat-inactivated  
194 fetal bovine serum (FBS; HyClone)] on dishes to allow the fibroblasts to grow out, the  
195 nerves were allowed to float in D-10+3M [DMEM, 10% FBS, 2  $\mu$ M forskolin (Sigma-  
196 Aldrich), 3.5  $\mu$ M heregulin (GenWay Biotech), 20  $\mu$ g/ml pituitary extract (Alfa Aesar),  
197 0.1% gentamycin (Thermo Fisher Scientific)]. After 10 days, the cells were then  
198 dissociated with enzymes [dispase, 12.5 U/ml (Thermo Fisher Scientific), collagenase,  
199 0.5% (Worthington Biochemicals)], plated, and allowed to grow to confluency before  
200 Thy1-complement treating to remove Thy1<sup>+</sup> fibroblasts. Subsequently, the passage one  
201 (P<sub>1</sub>) cells were expanded by either plating onto fresh poly-L-lysine (PLL; Sigma-Aldrich)  
202 coated 10 cm dishes or frozen for later use.

203

### 204 **2.2 Viral manipulation of SCs:**

205 Green fluorescent protein (GFP) and luciferase (luc) were used to identify the  
206 transplanted cells. SCs were transfected with lentiviruses (LV). LVs were produced by  
207 the Miami Project Viral Vector Core. Viruses were serially applied to the cells at the

beginning of each passage. Cells were exposed to the viruses for 18 - 20 hours. LV containing enhanced green fluorescent protein (LV-GFP; MOI 23) was applied to P<sub>1</sub> cells and resulted in 94.5% of SCs expressing GFP. LV containing luciferase (LV-luc; MOI 40) was added to P<sub>2</sub> cells already expressing GFP. A variety of LV-luc constructs were generated to detect light and examine HIF expression in SCs. High levels of luciferase activity were needed to generate enough light to penetrate through the muscle and skin above the transplant site. As a result, cells with the greatest luciferase expression were used. These cells expressed a control construct for examining HIF stabilization [ODD-luc-AYIA (Smirnova et al., 2010)]. To overexpress HIF-1 $\alpha$  in SCs, P<sub>3</sub> SCs expressing GFP and luc were transfected with a retrovirus expressing HIF in which HIF transcriptional activity is enhanced by the inclusion of the VP16 transactivation domain (RV-VP16-HIF; MOI 10) or a control virus (VP16; MOI 10) (Kung et al., 2000; Aminova et al., 2005). The viruses were previously generated by transfection of 293T cells with pBAB-puro-HIF-1 $\alpha$ -VP16 or a control plasmid (pBABE-puro-VP16) (Harvard Gene Therapy Initiative, Boston) and kindly provided by Dr. Rajiv Ratan. The RV-VP16-HIF virus results in the expression of a fusion protein encoding amino acids (aa) 1-529 of HIF-1 $\alpha$  and 78 aa of the VP16 transactivation domain (TAD). The VP16 TAD is a potent TAD located within the carboxyl-terminal of herpes simplex virus type 1 transcription factor VP16. When the VP16 TAD is fused to a transcription factor, it amplifies its activity. By creating a fusion protein with aa 1-529 of HIF-1 $\alpha$  that contains the DNA binding domains of HIF-1 $\alpha$ , but lacks the oxygen degradation domain, this virus produces a HIF-1 $\alpha$  fusion protein with both enhanced stability and transcriptional activity. Retroviruses were added in the presence of polybrene (4  $\mu$ g/ml). Cells were

231 subsequently expanded and frozen. For experiments, SCs between P<sub>4</sub> and P<sub>8</sub> were  
232 used.

233

### 234 **2.3 RNA isolation and PCR:**

235 RNA was collected from SCs by adding TRI reagent (Zymo Research) to the SCs  
236 and then isolating the RNA using the Direct-zol RNA Miniprep (Zymo Research)  
237 according to the manufacturer's instructions. To confirm viral expression of HIF, RNA  
238 was isolated. RNA was quantified using the Nanodrop spectrophotometer (Thermo  
239 Fisher Scientific). cDNA was generated using Superscript III First Stand Synthesis  
240 System (Thermo Fisher Scientific) and PCR was subsequently performed using primers  
241 for HIF-1 $\alpha$ , VP16 and  $\beta$ -actin (as per Aminova et al., 2005) and PCR products identified  
242 following electrophoresis.

243

### 244 **2.4 Protein isolation and western blotting:**

245 Nuclear and cytoplasmic proteins were isolated from cultured SCs using the NE-PER  
246 Kit (Thermo Fisher Scientific), as per the manufacturer's instructions. Cells were  
247 collected in CER I buffer with protease inhibitors by mechanically scraping. During  
248 isolation of the nuclear fraction, NaCl (200 mM; Sigma-Aldrich) was added at 10  
249 minutes to facilitate release of bound nuclear proteins and 1  $\mu$ l ( $\geq$  250 U) of benzonase  
250 nuclease (Sigma-Aldrich) was added at 20 minutes to digest nucleotides. Protein  
251 concentration was determined by DC assay, as per the manufacturer's instructions (Bio-  
252 Rad). For western blotting, the protein samples were quantified and either used  
253 immediately or stored at -80°C. Protein samples were heat-denatured (95 °C, 5 min),  
254 mixed with 6x loading buffer with SDS (Boston BioProducts), and loaded onto a 4-15%

255 gradient precast SDS Page gel (Bio-Rad). Using electrophoresis, proteins were  
 256 separated [120 V, 1.5 h, RT, running buffer (Boston BioProducts)], and subsequently  
 257 transferred to a nitrocellulose membrane [100 V, 1.5 h, 4 °C, transfer buffer (Boston  
 258 BioProducts)] with 20% methanol. Nuclear protein (50 µg), was assessed for HIF-1α  
 259 (1:1000, Novus NB 100-105) and HIF-2α (1:500, Novus NB 100-122). Nuclear protein  
 260 (20 µg) was assessed for VP16 (1:1000, ab4808, Abcam). Cytoplasmic protein (20 µg)  
 261 was assessed for VEGF (1:500, NB100-2381, Novus Biologicals) and enolase (1:1000,  
 262 NB100-65252, Novus Biologicals). β-actin (1:10 000, Sigma-Aldrich) or GFP (1:1000,  
 263 G6539, Sigma-Aldrich) was used as a loading control. Antibodies were diluted in  
 264 Odyssey blocking buffer (LI-COR). Primary antibodies were incubated overnight at 4°C.  
 265 LI-COR secondary antibodies (1:10 000; IRDye 800CW, IRDye 680LT) were incubated  
 266 for 90 min at room temperature. Membranes were imaged and band intensities were  
 267 quantified using the Odyssey Infrared Imaging System (LI-COR). For each antibody, a  
 268 minimum of three separate samples per condition were run and analyzed from the same  
 269 blot. For some experiments, SCs were treated for 24 h with 200 µM deferoxamine  
 270 (Sigma-Aldrich), a known HIF stabilizer. Samples from these cells were used as a  
 271 positive control for localization of HIF proteins on HIF western blots.

272

### 273 **2.5 *In vitro* cell death assays:**

274 To assess the effects of HIF on SC survival *in vitro*, LV-GFP-luc-VP16 HIF SCs  
 275 (VP16-HIF SCs) or LV-GFP-luc SCs (control) were plated onto 96-well plates and  
 276 grown for 41- 47 hours. Media was then removed and fresh D-10-3M was added along  
 277 with various inducers of cell death. Hydrogen peroxide (H<sub>2</sub>O<sub>2</sub>: 1-1000 µM, Sigma-  
 278 Aldrich) was added to dishes in which 10 000 SCs were plated to induce oxidative

279 damage. SC survival was assessed 3 h later. To determine the impact of other  
280 activators of cell death, 25 000 cells per well were plated and SC survival was assessed  
281 24 h later. Tunicamycin (0-8  $\mu$ M, Sigma-Aldrich) was added to activate the unfolded  
282 protein response. Thapsigargin (0-6  $\mu$ M, Sigma-Aldrich) was added to induce calcium  
283 release from intracellular stores. Camptothecin (0-12  $\mu$ M, Sigma-Aldrich) was added to  
284 induce DNA damage. SC survival was assessed by MTS assay (Promega). Phenazine  
285 methosulfate (PMS) was added to MTS [tetrazolium compound: 3-(4,5-dimethylthiazol-  
286 2-yl)-5-(3-carboxymethoxyphenyl)-2-(4-sulfophenyl)-2H-tetrazolium, inner salt]  
287 immediately prior to addition to the cells, as per the manufacturer's instructions. The  
288 media was replaced by MTS solution either 3 h ( $\text{H}_2\text{O}_2$  assays) or 24 h (all other assays)  
289 after treatment. Cells were incubated with MTS at 37°C, 6%  $\text{CO}_2$  for 4 h before  
290 absorbance was read using the SpectraMax i3 cytometer/spectrophotometer (Molecular  
291 Devices) at 490 nm. Percent survival was calculated for each condition per plate relative  
292 to untreated cells of the same type (VP16-HIF or control SCs). Briefly, the percentage of  
293 cells surviving in each well was calculated [(well absorbance - blank  
294 absorbance)/average absorbance of untreated cells]. Next, for each treatment for a  
295 given cell type on a given plate, the mean for the technical replicates was determined to  
296 establish the percent survival for each condition (i.e., each independent sample).  
297 Finally, percent survival per condition was calculated by averaging the results from each  
298 independent sample. Results represent the means of 3-4 independent assays in which  
299 the technical replicates (3-4/replicate) were averaged. For all assays, 2  $\mu$ l of lysis  
300 solution (9% weight/volume Triton X-100; Thermo Fisher Scientific) was added to  
301 assess maximal death.

302

## 303 2.6 SCI and Transplantation:

304 Female Fischer 344 rats (Harlan, barrier 217, 9-11 weeks of age) were  
305 anesthetized with isoflurane (2-3%). A laminectomy was performed to remove the  
306 dorsal process of thoracic vertebrae 9 (T9) to expose the spinal cord. The lateral  
307 processes of T8 and T10 were clamped and a 200 kdyn injury was induced using the  
308 Infinite Horizon impactor (Precision Systems and Instrumentation). The impact curve  
309 was checked for hit quality at the time of injury and saved. The injury site was inspected  
310 for a bruise prior to suturing the muscles closed in two separate anatomical layers. The  
311 skin was closed with wound clips. The temperature of the rats was monitored and  
312 maintained throughout the surgery using a thermoregulated heating pad. Buprenorphine  
313 (0.05 mg/kg) was given twice a day for the first two days post-surgery to alleviate pain.  
314 Lactated Ringer's (10 ml) was given 1 - 2 times per day for the first two days post-  
315 surgery to prevent dehydration. Gentamycin (5 mg/kg) was given once a day for the first  
316 7 days post-surgery to prevent infections. Along with food and water *ad libitum*, wet food  
317 pellets were provided to help maintain the rat's weight. Rats were housed in pairs, or in  
318 groups of three, and cages were placed on thermoregulated heating pads (half on-half  
319 off) to assist with thermoregulation for the first week post-surgery.

320 Seven days after SCI rats underwent a second surgery to transplant the cells. Rats  
321 were anesthetized with isoflurane (2-3%) or ketamine and xylazine (80 mg/kg:10  
322 mg/kg). The anesthetic used was kept consistent for each experiment. The previous  
323 incision site was reopened and the laminectomy site re-exposed. The dorsal vertebral  
324 process of T8 was clamped to stabilize the rat and 6  $\mu$ l of cells was injected into the  
325 injury site. Cells were injected using a pulled glass capillary tube with silicone plug  
326 attached to a Hamilton syringe affixed to a nanosyringe pump (KD Scientific) attached

327 to a stereotactic device. Cells were injected at a rate of 1  $\mu$ l/min at a depth of 1 - 1.25  
328 mm. The capillary was left in place for an additional 3 minutes to allow the pressure to  
329 equilibrate before removal. The laminectomy site was then sutured closed in two  
330 anatomical layers and the skin was closed with wound clips. Surgical and post-surgical  
331 care (e.g., temperature monitoring, drugs) was administered as after the initial SCI  
332 surgery. All animal procedures were performed in accordance with the Weill Cornell  
333 Medical College animal care committee's regulations.

334

### 335 **2.7 Optimization of *in vivo* bioluminescent imaging (IVIS):**

336 To examine transplant survival in rats over time, and to assess whether IVIS imaging  
337 could be used to measure transplant survival more rapidly than stereological  
338 quantification, changes in light emission over the first 7 days following transplantation  
339 were quantified using the IVIS 100 (PerkinElmer). Initial experiments examined the  
340 sensitivity of the IVIS for detecting different numbers of transplanted cells and compared  
341 intraperitoneal injection of d-luciferin with intravenous injection following transplantation  
342 of  $2 \times 10^6$  GFP-luc SCs. Intravenous administration via the tail vein resulted in a more  
343 rapid increase in light production than intraperitoneal administration (not shown). The  
344 time course of the decrease in light emitted from the transplants over time was  
345 compared to the number of transplanted cells at 3 days (n=4) and 7 days (n=5). A  
346 subset of these rats were quantified by stereology to determine the number of surviving  
347 SCs at 3 days (n=3) and 7 days (n=4). Spinal cords from two of the rats that underwent  
348 IVIS imaging were not available for histological analysis.

349

### 350 **2.8 Transplantation of HIF-1 $\alpha$ SCs and assessments of transplant survival:**



351 To assess whether increasing HIF-1 $\alpha$  in SCs promoted transplanted SC survival, the  
352 effect of overexpressing HIF was tested in a fully-blinded, randomized, *in vivo* SCI  
353 experiment. Both the treatment group assignment and the order of the cell types  
354 transplanted were assigned randomly prior to cell collection and transplantation.  
355 Twenty-six rats underwent a T9, 200 kdyn IH SCI (one rat died post-SCI). The 25  
356 remaining rats received SC transplants 7 days post-SCI and were euthanized at 7 days  
357 post-TP (14 dpi). Rats received transplants of  $2 \times 10^6$  SCs directly into the injury  
358 epicenter. The three transplant treatment groups were: GFP-luc SCs (control SCs, n=9);  
359 GFP-luc-VP16-SCs (VP16 SCs, n=8), and; GFP-luc-VP16-HIF-1 $\alpha$  SCs (VP16-HIF SCs,  
360 n=8). Using up to three different methods, transplant survival was assessed in the same  
361 rats. Following transplantation, 12 of the 25 rats (n=4/group) underwent *in vivo*  
362 bioluminescent imaging using the IVIS Spectrum (PerkinElmer) to detect the  
363 transplanted cells based on their luciferase expression. *In vivo* bioluminescent imaging  
364 was performed on these 12 rats daily for the first 3 days post-TP—the time window in  
365 which we determined that transplanted cell death occurs. Seven days post-TP, after  
366 perfusion and isolation of the spinal cords (n=25), *ex vivo* GFP fluorescent imaging of  
367 the spinal cords was performed using the IVIS Spectrum. The spinal cords were then  
368 sectioned with a cryostat and the number of surviving SCs was quantified by Stereo  
369 Investigator (MBF Bioscience). By sequentially assessing the same spinal cords, we  
370 were able to compare non-biased stereology, which reliably detects differences in  
371 transplant survival, with alternative methods of transplant survival quantification. In this  
372 study, we compared the results of the stereological quantification of surviving SCs with  
373 *ex vivo* fluorescent imaging of light emission from GFP and *in vivo* bioluminescent  
374 imaging of luciferase activity within a single set of experimental rats. Upon histological



375 inspection of the 25 spinal cords, 21 rats were determined to have received good  
376 transplants (SCs n=7; VP16 n=6; VP16-HIF SCs n=8) and were included in the  
377 stereological and *ex vivo* imaging analyses. For *in vivo* bioluminescence, all imaged rats  
378 that were determined to have received good transplants were included in the analysis  
379 (SCs n=3; VP16 n=4; VP16-HIF SCs n=4).

380 Exclusion of rats from the analysis was based on assessment of the quality of the  
381 transplant, which was undertaken prior to unblinding of the experiment. The transplants  
382 were assessed histologically for tissue section completeness and location of the  
383 transplanted cells in both the rostral-caudal and dorsal-ventral axes relative to the lesion  
384 epicenter. The stereological results were then compared with the transplant surgery  
385 notes and notes on the histological assessment of the transplants. Two rats with small  
386 transplants were excluded because of problems with the injection that were noted at the  
387 time of transplantation. Two additional rats were excluded because the transplant was  
388 not located within the lesion epicenter.

389

## 390 **2.9 IVIS luminescent imaging:**

391 IVIS luminescent imaging was performed using either the IVIS 100 or IVIS Spectrum.  
392 Rats were anaesthetized with isoflurane (1-2%; Henry Schein). Baseline images were  
393 acquired prior to intravenous injection of d-luciferin (150 mg/kg, Gold Biotechnology)  
394 into the tail vein. IVIS imaging was performed daily as close as possible to the time of  
395 transplantation each day. Following administration of d-luciferin, IVIS images were  
396 acquired by collecting the amount of light emitted over 5 minutes (Exposure: 5 minutes;  
397 Binning: medium; F/stop: 1; Field of view: 400 cm<sup>2</sup>; Emission filter: open). Rats were  
398 imaged continuously in 5-minute intervals for up to 60 minutes to determine the time of

399 maximum light emission. The image with maximum light was used to quantify the  
400 amount of light emitted. A region of interest (ROI) of 6.41 cm<sup>2</sup> was centered over the  
401 site of maximum light and both the average radiance (photons/s/cm<sup>2</sup>/steradian) and the  
402 total flux (photons/s) were determined. Because total flux is derived from average  
403 radiance, results from both showed a similar profile. Average radiance is presented. In  
404 cases where light was not initially detected within 0 – 30 minutes, rats received a  
405 second injection of d-luciferin and were re-imaged. If, following a second injection, light  
406 was not detected, the data was excluded from analysis for that time point only.

407

#### 408 **2.10 Tissue collection:**

409 Three days (n=3) or seven days (total, n=29; assessment of timing of death, n=4;  
410 assessment of VP16-HIF SC transplants, n=25) after transplantation, rats were  
411 sacrificed by lethal injection of ketamine (Henry Schein)/xylazine (Henry Schein). Spinal  
412 cords were collected after trans-cardiac perfusion of heparinized (Henry Schein) 0.9%  
413 saline followed by 4% paraformaldehyde (Sigma-Aldrich). Paraformaldehyde-fixed  
414 tissue was post-fixed overnight before transferring to 30% sucrose-PBS (Sigma-Aldrich)  
415 to facilitate cryopreservation for histological analysis.

416

#### 417 **2.11 *Ex vivo* IVIS fluorescent imaging:**

418 The amount of fluorescent light emitted from the GFP transplants was quantified in  
419 the isolated fixed spinal cords using *ex vivo* imaging with the IVIS Spectrum. Spinal  
420 cords were placed on a petri-dish with a black backing and inserted into the IVIS  
421 Spectrum. The number of photons emitted by the GFP<sup>+</sup> SCs within the spinal cord was  
422 determined using the following IVIS settings: excitation/emission = 500/540; exposure =

423 0.5 s; binning = 4, F-stop = 2; field of view = B. A photographic image of the spinal cord  
424 overlaid with the photon intensity count was generated. The ROI of GFP fluorescence  
425 was then auto-sized and the average radiant efficiency  $[(p/s/cm^2/sr)/(\mu W/cm^2)]$   
426 determined for each case. To account for variability in light intensity between images,  
427 the same settings were used to show visible photons on all the images (Min =  $3.25 \times$   
428  $10^8$ ; Max =  $10 \times 10^9$ ).

## 430 **2.12 Histology and quantification of SC survival and transplant volume:**

431 A 15 mm block of the spinal cord containing the injury epicenter was cut into  
432 longitudinal sections (20  $\mu m$ ) on the cryostat. Four sets of serial sections were collected  
433 onto charged slides. Nuclei were labeled by incubating tissue sections with 1:1000  
434 Hoechst (Sigma-Aldrich) in PBS (pH 7.4) for 1 h. Slides were air dried and coverslipped  
435 with Vectashield (Vector Laboratories) prior to imaging. To quantify the total number of  
436 transplanted GFP<sup>+</sup> SCs and the GFP<sup>+</sup> transplant volume, Stereo Investigator was used.  
437 The transplant was outlined at 10x magnification. Using the Cavalieri function,  
438 transplant volume was quantified at 10x magnification (grid size was 200 x 200  $\mu m$ ).  
439 Using the optical fractionator function, the number of GFP<sup>+</sup> cells were quantified at 63x  
440 magnification (grid box size was 150 x 400  $\mu m$  and the sampling box was 50 x 50  $\mu m$ ).

## 442 **2.13 Imaging:**

443 Tissue was examined, imaged, and quantified using either a Zeiss Axiovert 200M or  
444 a Zeiss AxioImager M2 equipped with Stereo Investigator. Virtual tissue sections were  
445 acquired at 10x magnification. Similar Exposure and Gain settings were maintained for

all image acquisition for a given experiment. Confocal images were acquired using a Zeiss LSM 510 META confocal microscope.

#### 2.14 Chemical and Biosafety:

All viral work was performed using biosafety level 2 procedures and approved by the Weill Cornell Medical College Institutional Biosafety Committee. Individuals working with viruses and chemicals received institutional biosafety and chemical training and donned appropriate personal protective equipment when executing experiments with hazardous material.

#### 2.15 Statistics:

All statistics were performed using SPSS (Version 22; IBM). An overview of statistical tests used can be found in Table 1. Specifics of the statistical tests used are included in the results.

Table 1. Statistical Table

	Data structure	Type of test	Power
a	Normal distribution	Univariate Analysis of Variance, Repeated Contrasts	0.89
b	Normal distribution	t-test	0.08
c	Normal distribution	Univariate Analysis of Variance	1.00
d	Normal distribution	Univariate Analysis of Variance	0.14
e	Normal distribution	Univariate Analysis of Variance	1.00
f	Normal distribution	Univariate Analysis of Variance	1.00
g	Normal distribution	Univariate Analysis of Variance	1.00
h	Normal distribution	Univariate Analysis of Variance	0.94
i	Normal distribution	Univariate Analysis of Variance	1.00
j	Normal distribution	Univariate Analysis of Variance	0.95
k	Normal distribution	Univariate Analysis of Variance	1.00
l	Normal distribution	Univariate Analysis of Variance	0.22
m	Normal distribution	Univariate Analysis of Variance	1.00
n	Normal distribution	Univariate Analysis of Variance	0.85
o	Normal distribution	Univariate Analysis of Variance	0.76
p	Normal distribution	Univariate Analysis of Variance	0.43

q	Normal distribution	Univariate Analysis of Variance, Repeated Contrasts	0.89
r	Normal distribution	Univariate Analysis of Variance	0.43
s	Normal distribution	General Linear Model	0.53

463

464 **3. RESULTS**465 **3.1 Transplanted cell number does not change between 2 and 7 days post-**  
466 **transplant**

467 Transplanted cells die early after transplantation into the injured spinal cord (Barakat  
468 et al., 2005; Hill et al., 2006; Karimi-Abdolrezaee et al., 2006; Hill et al., 2007). However,  
469 the exact time course of transplanted cell death remains to be established. To  
470 counteract transplanted cell death, it is necessary to establish the window in which the  
471 death occurs. Several studies have shown that the amount of light detected using  
472 bioluminescent imaging correlates with cell number transplanted and that the light  
473 decreases following the transplantation of cells (Okada et al., 2005; Takahashi et al.,  
474 2011; Roet et al., 2012; Nishimura et al., 2013). Using the IVIS imaging system,  
475 bioluminescent imaging was performed for either 7 days (n=4) or 3 days (n=3) to  
476 establish when post-TP transplanted cells die. Following intravenous injection of d-  
477 luciferin via the tail vein, it took 5-10 minutes for the amount of detected light to reach  
478 the maximal level, as measured by average radiance. The maximal amount of light  
479 produced by the luciferase-expressing SCs decreased significantly over time post-TP  
480 [univariate ANOVA:  $F(6, 36) = 3.302$ ,  $p=0.011^a$ ]. The amount of light detected at day 2  
481 was significantly lower than on day 1 (K Matrix: 1d vs 2d,  $p=0.004^a$ ). After day 2, no  
482 further reduction in light production was detected. The amount of light detected was  
483 similar from 2-7 days post-TP (K Matrix: all other contrast  $p>0.05^a$ ; days 2-7: Ryan-  
484 Einot-Gabriel-Welsch homogenous subset,  $p=0.98^a$ ) (Fig. 1A). Thus, based on the

485 amount of light detected by *in vivo* bioluminescent imaging, we established that the  
486 number of transplanted cells decreases within the first 48 hours post-TP.

487 To confirm that the number of surviving transplanted cells did not differ after the first  
488 few days, when the light levels in the IVIS had plateaued, the spinal cords from the IVIS  
489 imaged rats were examined histologically. The number of GFP<sup>+</sup> SCs within the  
490 transplants were quantified at 3 (n=3) and 7 days (n=4) post-TP. Stereological  
491 quantification confirmed that the number of surviving transplanted SCs did not differ  
492 between 3 d and 7 d post-TP (Fig. 1B; t-test, df:5, p=0.8<sup>b</sup>). This fits with previous work in  
493 which necrosis and apoptosis of transplanted SCs was detected at 24 h but not 3 days  
494 post-TP (Hill et al., 2007). These experiments led us to conclude that the death of the  
495 cells occurs within a narrow time window immediately post-TP and concludes within 2-3  
496 days.

497 Multiple factors are postulated to contribute to transplanted cell death (e.g., cell  
498 processing, transplant procedure, injury/transplant environment, transplant rejection).  
499 Examination of the factors that contribute to transplanted cell death indicate that the  
500 injury/transplant environment is the likely culprit (Hill et al., 2006; Hill et al., 2007; Hill et  
501 al., 2010). Cell processing and the transplant procedure account for less than 10% of  
502 the observed cell death (Hill et al., 2007). In a model of transplant rejection,  
503 immunosuppression does not block this early death (Hill et al., 2006). Transplant  
504 survival is enhanced by delaying engraftment for at least 7 days (McDonald et al., 1999;  
505 Hill et al., 2006), but is not further augmented by waiting for the chronic injury site to  
506 develop (Barakat et al., 2005). This suggests that the environment generated by the cell  
507 transplant is a key contributor to acute transplanted cell death, and likely why cell death  
508 is a common feature of all cell transplants.

509

510 **3.2 Expression of VP16-HIF-1 $\alpha$  in SCs increases HIF-1 $\alpha$ , but not HIF-2 $\alpha$ , and**  
 511 **increases protein expression of HIF target genes**

512 Although the exact cause of this death has not been established, the complexity and  
 513 redundancy of the pathways involved in tissue damage after SCI support targeting  
 514 coordinated responses instead of a single gene, protein, or pathway in order to improve  
 515 transplant survival. Activation of transcriptional programs leads to alterations in targeted  
 516 downstream cassettes of genes which act in concert to alleviate the relevant stress(es)  
 517 and their by-products. Harnessing the power of cellular transcriptional programs could  
 518 abrogate the need to identify and target individual cell death inducers.

519 Hypoxia-inducible factor 1 $\alpha$  (HIF-1 $\alpha$ ) is a member of a family of transcription factors  
 520 that regulate transcriptional responses involved in cellular metabolism and wound  
 521 healing (Ruthenborg et al., 2014; Yang et al., 2014; Pugh, 2016). HIF target genes are  
 522 involved in cell growth and fate, mitochondrial functioning, glycolysis and glucose  
 523 metabolism, and oxygen transport and delivery (Semenza, 2012), all of which could  
 524 benefit transplanted cell survival. In the current series of experiments, we sought to  
 525 elevate HIF-1 $\alpha$  in SCs and test whether it could promote the survival of the transplanted  
 526 cells.

527 Experimentally, HIF-1 $\alpha$  levels can be manipulated genetically by the generation of  
 528 non-hydroxylatable HIF-1 $\alpha$  (Kung et al., 2000; Aminova et al., 2005). Using a retrovirus  
 529 to express a VP16-HIF-1 $\alpha$  fusion protein that contains a transcriptionally-active, non-  
 530 degradable form of HIF-1 $\alpha$  (Kung et al., 2000; Aminova et al., 2005), we elevated HIF-  
 531 1 $\alpha$  levels in SCs to physiological levels. Following transduction of SCs with retroviruses  
 532 expressing either VP16-HIF-1 $\alpha$  or VP16, VP16 mRNA (Fig. 2A) and protein (Fig. 2B, C)

533 were detected in both VP16 and VP16-HIF SCs. Human HIF-1 $\alpha$  mRNA (Fig. 2A) was  
 534 detected in VP16-HIF-1 $\alpha$  SCs but not VP16 SCs. At the protein level, HIF-1 $\alpha$  (Fig. 2B,  
 535 D), but not the closely-related HIF-2 $\alpha$  (Fig. 2B, E), was significantly elevated in VP16-  
 536 HIF-1 $\alpha$  SCs [HIF-1 $\alpha$ : ANOVA:  $F(6,2)=7993.5$ ,  $p<0.0001^c$ , Bonferroni post-hoc,  
 537  $p<0.0001$ ; HIF-2  $\alpha$ : ANOVA:  $F(6,2)=0.878$ ,  $p=0.463^d$ ], thus demonstrating the specificity  
 538 of the virus for HIF-1 $\alpha$ . Compared to control SCs, HIF-1 $\alpha$  levels were increased by  $5.9 \pm$   
 539  $0.2$  fold in VP16-HIF SCs. This is within the physiological increase in HIF-1 $\alpha$  achieved  
 540 with hypoxia treatment in other cell types [e.g., stem cells: (Theus et al., 2008; Wakai et  
 541 al., 2016); bone marrow stromal cells (BMSCs; Theus et al., 2008)], where HIF-1 $\alpha$   
 542 increases by 2- to 6.5-fold. It is, however, less than the 8-14-fold increase achievable  
 543 following pharmacological treatment of SCs with the HIF stabilizer, deferoxamine  
 544 (unpublished data). Expression of VP16-HIF in SCs resulted in the elevation of two  
 545 representative HIF target genes: VEGF, a protein important in tissue vascularization,  
 546 and enolase, a glycolytic enzyme. VEGF increased  $2.2 \pm 0.2$  fold [Fig. 2B, F: ANOVA:  
 547  $F(6,2)=3223.6$ ,  $p<0.0001^e$ , Bonferroni post-hoc,  $p<0.0001$ ]. Enolase increased  $1.7 \pm$   
 548  $0.01$  fold [Fig. 2B, G: ANOVA:  $F(6,2)=277.1$ ,  $p<0.0001^f$ , Bonferroni post-hoc,  $p<0.0001$ ].  
 549 Thus, retroviral expression of a non-degradable form of HIF-1 $\alpha$  fused to the VP16-  
 550 transactivation domain elevated HIF-1 $\alpha$  levels in SCs to the physiological levels, and  
 551 was sufficient to elevate the expression of HIF's transcriptional targets. The level of  
 552 expression, while within the physiological range, was sub-maximal.

553

554 **3.3 Elevation of HIF in SCs via retroviral expression of VP16 HIF enhances SC**  
 555 **survival in response to oxidative stress, but not ER stress or DNA damage.**



556 The transcriptome regulated by HIF contains a core set of genes activated in response  
557 to hypoxia (Benita et al., 2009), along with cell-specific transcriptional changes (Chi et  
558 al., 2006). This generates both specificity and diversity in the transcriptional response  
559 (Lendahl et al., 2009). Activation of HIF adaptive signaling is primarily associated with  
560 cytoprotection, as evidenced by its protective effect on transplanted cells when elevated  
561 either directly or indirectly by induction with hypoxia or pharmacological preconditioning  
562 (Chu et al., 2008; Theus et al., 2008; Wu et al., 2010). However, among HIF's target  
563 genes are BNIP3 and NIX, which are associated with mitochondrial damage, apoptosis  
564 and autophagy (Ney, 2015). Moreover, in a neuronal cell line *in vitro*, HIF expression  
565 augments glutamate-induced oxidative stress-mediated cell death (Aminova et al.,  
566 2005). Thus, at least in some contexts, elevation of HIF-1 $\alpha$  can lead to enhancement of  
567 cell death.

568 To determine whether expression of HIF-1 $\alpha$  was cytoprotective for SCs against  
569 oxidative stress-induced cell death, the effects of overexpression of HIF-1 $\alpha$  on cell  
570 survival was assessed *in vitro* by MTS assay. To model oxidative damage *in vitro*, SCs  
571 were exposed to hydrogen peroxide (0-1000  $\mu$ M) for 3 hours. This dose range resulted  
572 in a dose-dependent reduction in SC survival from 0-150  $\mu$ M H<sub>2</sub>O<sub>2</sub> [ANOVA: F(9,  
573 40)=246.1, p<0.0001<sup>g</sup>; K matrix: 0-150  $\mu$ M, p<0.05]. There were significantly more  
574 VP16-HIF SCs compared to control SCs across a range of H<sub>2</sub>O<sub>2</sub> concentrations (Fig.  
575 3A: 3.9, 15.6, 31.3, 62.5  $\mu$ M) [ANOVA: F(1,40)=12.9, p=0.001<sup>h</sup>, post-hoc: Fisher's LSD,  
576 p $\leq$ 0.05]. The extent by which HIF-1 $\alpha$  protected the SCs varied with H<sub>2</sub>O<sub>2</sub> concentration.  
577 At the LD50 dose of H<sub>2</sub>O<sub>2</sub>, 31.5  $\mu$ M, 45.2%  $\pm$  4.58% of control SCs survived, whereas  
578 62.8%  $\pm$  4.64% of VP16-HIF SCs survived. Expression of HIF-1 $\alpha$  increased SC survival  
579 by 39%. This is equivalent to the protection achieved by calpain inhibition (Hill et al.,

2010). Therefore, expression of HIF-1 $\alpha$  in SCs was sufficient to protect SCs against oxidative stress-mediated cell death. These results were expected, given HIF-1 $\alpha$ 's established role in mitigating reactive oxygen species-mediated damage (reviewed in Thomas and Ashcroft, 2019), but were contrary to the results found in a neuronal cell line (Aminova et al., 2005).

Under some contexts, HIF expression can be deleterious (Aminova et al., 2005). The effects are both cell type (Vangeison et al., 2008) and injury inducer-dependent (Aminova et al., 2005). As the inducers of transplanted cell death remain to be identified, we further examined the survival of SCs by evaluating their survival *in vitro* in response to several additional known inducers of cellular toxicity, including: DNA damage, ER stress, and protein unfolding to establish the context in which HIF-1 $\alpha$  leads to SC cytoprotection.

To assess the ability of HIF to protect SCs against DNA damage, SCs were exposed to camptothecin (0-12  $\mu$ M) *in vitro* for 24 h (Fig. 3B). Camptothecin significantly reduced the viability of SCs across the range of concentrations tested [ANOVA: F(6,28)=8.5,  $p<0.0001$ ]. However, despite using a range of concentrations effective in other cells *in vitro* (Aminova et al., 2005), most of the SCs (80-87%) remained viable. Only 0.375  $\mu$ M camptothecin treatment differed from the preceding concentration (K-matrix: 0  $\mu$ M vs 0.375  $\mu$ M,  $p<0.0001$ , all other contrast  $p>0.05$ ; 0.375-12  $\mu$ M). The lack of a dose response curve across a range of concentrations that are toxic for HT22 cells indicates that SCs are relatively resistant to DNA damage-induced death via camptothecin. Although the effect of camptothecin on SC viability was modest, HIF expression protected SCs against camptothecin-mediated cell death [ANOVA: F(1, 28)=13.7,  $p=0.001$ ]. Viability of VP16-HIF SCs was significantly enhanced in response to

604 application of 3  $\mu$ M or 12  $\mu$ M camptothecin (post-hoc: Fisher's LSD, 3  $\mu$ M,  $p=0.002$ , 12  
605  $\mu$ M,  $p=0.014$ ). At 3  $\mu$ M, HIF-1 $\alpha$  increased cell survival by 17.7% — 79.4%  $\pm$  1.38% of  
606 control SCs survived compared to 93.5  $\pm$  7.31% of HIF-1 $\alpha$  SCs. At 12  $\mu$ M, HIF-1 $\alpha$   
607 increased survival by 12.5% — 83.9  $\pm$  1.35% of control SCs survived compared to 94.4  
608  $\pm$  2.34% of HIF-1 $\alpha$  SCs. Thus, although SCs are relatively resistant to DNA damage-  
609 induced cell death, elevating HIF is still sufficient to afford some protection to SCs  
610 against DNA damage-induced death.

611 ER stress was induced by exposure of SCs to thapsigargin (0-6  $\mu$ M; Fig. 3C) for 24h  
612 (Fig. 3C), which results in Ca<sup>++</sup> release from intracellular stores. Thapsigargin  
613 significantly altered SC viability across a range of concentrations [ANOVA:  
614  $F(5,24)=9.26$ ,  $p<0.0001^k$ ]; however, across concentrations proven toxic for HT22 cells  
615 (Aminova et al., 2005), SCs did not show a dose response curve and an LD50 was not  
616 obtained. Thapsigargin decreased cell viability to 88-93% of control at high doses (>1.5  
617  $\mu$ M). Unexpectedly, at low doses (0.375-0.75  $\mu$ M), thapsigargin increased cell viability to  
618 107-117% of control (0  $\mu$ M). Although not tested, this is likely due to altered SC  
619 proliferation. Only application of 0.375 and 1.5  $\mu$ M thapsigargin resulted in changes in  
620 viability relative to the preceding concentration (K matrix: 0 vs 0.375  $\mu$ M,  $p=0.002$ ; 0.75  
621 vs 1.5,  $p=0.02$ ). Based on the relatively small decrease in SC viability across a range of  
622 thapsigargin concentrations that are toxic to other cells, it appears that SCs were  
623 relatively resistant to ER stress induced by thapsigargin. Elevating HIF in SCs did not  
624 alter SC viability in response to thapsigargin [ANOVA:  $F(5,1)=1.5$ ,  $p=0.225^l$ ]. Larger  
625 alterations in SC survival in response to ER stress are needed to establish whether HIF-  
626 1 $\alpha$  levels impact ER stress-mediated cell death in SCs.

627 Accumulation of misfolded or unfolded proteins can lead to cell death. To induce  
628 protein unfolding in SCs, tunicamycin (0-8  $\mu$ M) was administered for 24 h (Fig. 3D).  
629 Administration of tunicamycin induces autophagy, which can either be protective, or, if  
630 autophagy is excessively activated or disrupted, lead to cell death (Ding et al., 2007).  
631 Tunicamycin administration resulted in a dose-dependent decrease in SC viability  
632 [ANOVA:  $F(5,24)=82.7$ ,  $p<0.0001^m$ ], but only at the lowest concentrations tested. There  
633 was a significant decrease in viability from the preceding tunicamycin concentration at  
634 0.5 and 1  $\mu$ M (K matrix: 0.5 vs 0  $\mu$ M,  $p<0.005$ ; 1 vs 0.5,  $p=0.04$ ). Beyond 1  $\mu$ M, at  
635 concentrations that are toxic to HT22 cells (Aminova et al., 2005), 59-63% of SCs  
636 continued to survive (Fig. 3D), indicating that SCs were relatively resistant to  
637 tunicamycin treatment. Expression of HIF-1 $\alpha$  in VP16-HIF SCs did not counteract the  
638 reduction in SC viability in response to tunicamycin. Rather, VP16-HIF SCs had a small  
639 reduction in viability compared to control SCs [ANOVA:  $F(1, 24)=9.7$ ,  $p=0.005^n$ ]. This  
640 significant difference was detected at only a single concentration (post-hoc: Fisher's  
641 LSD, 1  $\mu$ M,  $p=0.04$ ). At 1  $\mu$ M tunicamycin, HIF expression decreased SC viability by  
642 13.3% — 62.7%  $\pm$  1.11% of control SCs survived compared to 54.5%  $\pm$  2.69% of VP16-  
643 HIF SCs. Although a significant decrease in survival was observed when HIF-  
644 expressing SCs were treated with tunicamycin, the effect was restricted to a small  
645 change at a single dose of the 5 doses tested. Overall, SCs were relatively resistant to  
646 cell death induced by activation of the unfolded protein response. This likely reflects the  
647 importance of autophagy in the de-differentiation and reprogramming SCs (Gomez-  
648 Sanchez et al., 2015).

649 Previous reports indicate that the effects of HIF-1 $\alpha$  on cell survival are influenced by  
650 both the cell type and cell death mechanism (Aminova et al., 2005). In SCs, the *in vitro*

assays indicate that elevation of HIF via retroviral expression of VP16-HIF-1 $\alpha$  results in substantial protection against oxidative stress (38.9% increase). In other models of cell stress, the ability of elevated HIF-1 $\alpha$  in SCs to protect SCs was more variable and of a limited magnitude (< 20% increase or decrease). In SCs, HIF-1 $\alpha$  resulted in modest protection (DNA damage), no alteration (ER stress), or a reduction (unfolded protein response) in survival. These results fit with the overall view that activation of HIF-1 $\alpha$  adaptive pathways is cytoprotective, but that its effects are context-dependent.

### 3.4 Elevation of HIF in SCs via retroviral expression of VP16 HIF promotes transplanted SC survival 7 days post-transplantation)

Having established that expression of HIF-1 $\alpha$  in SCs led to elevated levels of target genes in adaptive HIF pathways (Fig. 2), and that this protected SCs against oxidative stress-induced cell death *in vitro* (Fig. 3A), we tested whether elevating HIF in SCs enhances their survival following transplantation into the injured spinal cord.

Following transplantation of SCs into the injured spinal cord 7 dpi, stereological quantification determined that significantly more SCs survived when VP16-HIF was expressed [number of surviving SCs: control, 128 400  $\pm$  18 900; VP16, 142 200  $\pm$  30 200, and; VP16-HIF: 172 400  $\pm$  30 100; ANOVA: F(18,2)=5.259, p=0.016<sup>o</sup>; post-hoc: 1-tail Fisher's LSD, control, p=0.0025, VP16, p=0.0265]. The increase in survival by 34.3% in VP16-HIF SCs compared to control SCs reflects a very large effect size (Hedges' g=1.72). The 21.2% increase in survival compared to VP16 SCs reflects a large effect size (Hedges' g=1.00). As many studies have assessed transplant size as a measure of transplant survival, we also quantified transplant volume. Transplantation of VP16-HIF SCs was associated with a slight, but significant, increase in transplant

675 volume relative to control SCs, but not VP16 SCs [transplant volume: control,  $1.6 \pm 0.15$   
676  $\text{mm}^3$ , VP16,  $1.9 \pm 0.29 \text{ mm}^3$ , VP16-HIF,  $2.1 \pm 0.47 \text{ mm}^3$ ; ANOVA:  $F(18,2)=5.162$ ,  
677  $p=0.016^p$ ; post-hoc: 1-tail Fisher's LSD, control,  $p=0.0025$ , VP16,  $p=0.11$ ]. The  
678 transplant volumes for all groups were within the size of SC transplants reported  
679 previously (Golden et al., 2007; Hill et al., 2010). The improvement of transplant survival  
680 achieved with HIF SCs is similar to that observed in some studies (Theus et al., 2008;  
681 Wang et al., 2018) in which HIF-1 $\alpha$  is targeted in either neural stem cell/progenitor cell  
682 or BMSC transplants.

683 HIF is associated with enhanced migration of cancer cells (Araos et al., 2018) and  
684 neural crest cells (Barriga et al., 2013). Larger transplants could arise from better  
685 transplant survival and/or enhanced transplant migration. No evidence for migration of  
686 the SCs out of the transplants and across the SC-astrocyte boundary were detected in  
687 this study. The presence of astrocytes and inhibitory molecules within the glial scar is  
688 known to prevent SC migration (Afshari et al., 2010).

689 In this study, we sought to test whether the elevation of HIF-1 $\alpha$  and activation of its  
690 transcriptional programs could provide an alternative approach to the use of  
691 preconditioning or growth factor augmentation for promoting the survival of the  
692 transplanted cells. Elevating the expression of HIF-1 $\alpha$  by 5.9-fold increased the  
693 expression of the HIF target genes VEGF and enolase by 2.2 and 1.7-fold, respectively.  
694 This level of HIF activity was associated with a 20 – 35% increase in transplant survival.  
695 Thus, we demonstrate that overexpression of a single transcription factor is sufficient to  
696 protect SCs transplanted into the injured spinal cord. Further optimization is needed to  
697 obtain the level of protection afforded by HIF-1 $\alpha$  in other transplant models either alone  
698 (Wu et al., 2010; Wakai et al., 2016) or with the inclusion of growth factors along with

699 cell transplants into the injured spinal cord (Golden et al., 2007; Lu et al., 2012;  
700 Robinson and Lu, 2017).

701

702 **3.5 *Ex vivo* fluorescent imaging of spinal cords and *in vivo* luminescent imaging**  
703 **of rats did not detect differences in transplant survival.**

704 A barrier to the development and identification of new strategies that promote cell  
705 survival are the methods currently used to assess transplant survival accurately. As part  
706 of this study, we assessed whether *ex vivo* fluorescent imaging (Fig. 3H, I) or *in vivo*  
707 bioluminescence imaging (Fig. 3J, K) could detect a difference in transplant survival.  
708 Similar to the earlier experiment, IVIS imaging was sensitive enough to detect a  
709 difference in light emission over time [ANOVA:  $F(8.89, 1.111)=11.955$ ,  $p=0.006^q$ ,  
710 sphericity corrected; post-hoc: Bonferroni, d1 vs d2,  $p=0.01$ , d1 vs d3,  $p=0.031$ ]. Neither  
711 IVIS imaging of live animals, nor *ex vivo* imaging of isolated spinal cords, was sensitive  
712 enough to detect the increase in transplant survival observed histologically [*ex vivo* IVIS  
713 GFP: ANOVA:  $F(18,2)=2.448$ ,  $p=0.115^r$ ; *in vivo* IVIS luciferase: ANOVA:  $F(8,2)=0.032$ ,  
714  $p=0.969^s$ ]. Based on power analyses, a minimum of 14 – 18 rats would be needed to  
715 detect a significant difference (power=0.8,  $\alpha=0.05$ ) between the three groups using  
716 either luminescence or GFP as an outcome on the IVIS, respectively. Although *ex vivo*  
717 and *in vivo* imaging of the transplants is feasible; a large number of samples would be  
718 needed to reliably detect differences. Thus, these methods are unlikely to be a more  
719 rapid alternative to stereological quantification of transplanted cells.

720

721 **4. DISCUSSION**



722 The results of the current studies establish that transplanted cells die prior to 2 days  
723 post-TP. The narrow window of cell death followed by the stabilization of the number of  
724 transplanted cells supports that acute, rather than prolonged, manipulation of survival  
725 pathways could be sufficient to counteract transplanted cell death. HIF-1 $\alpha$  is involved in  
726 cellular adaptations to stress. Here, we demonstrate that the elevation of HIF-1 $\alpha$   
727 increases cell survival in both an *in vitro* model of transplanted cell injury and following  
728 transplantation of SCs into the sub-acutely injured spinal cord. We show that  
729 stabilization of HIF-1 $\alpha$  elevates HIF transcriptional targets and is sufficient to protect  
730 SCs against oxidative stress and DNA damage-induced cell death, two major  
731 mechanisms of cell death following SCI (Ahuja et al., 2017). When HIF-1 $\alpha$ -expressing  
732 SCs are transplanted into the injured spinal cord, where multiple inducers of cell death  
733 are present (Ahuja et al., 2017), more cells survive. These experiments support the  
734 utility of harnessing cellular adaptive responses in order to protect them from  
735 subsequent transplant-induced cellular stress. They also establish that targeting a  
736 transcription factor (HIF-1 $\alpha$ ) and activation of its target pathways is cytoprotective for  
737 cells transplanted into the injured spinal cord. This identifies an alternative approach to  
738 those currently used which target individual cell death inducers or signaling pathways,  
739 or involve the inclusion of multiple growth factors along with the transplanted cells.  
740 Importantly, strategies exist to transiently elevate HIF-1 $\alpha$  transcriptional programs (e.g.,  
741 hypoxic preconditioning or pharmacological pretreatment of transplanted cells), which, if  
742 effective, will enable the elevation of protective transcriptional programs using a  
743 pretreatment approach. Pretreatment of the cells could provide a more clinically-feasible  
744 method for enhancing transplant survival than current pro-survival approaches, which  
745 require inclusion of multiple proteins along with the cells.



746        Histological quantification of transplant survival is laborious. The identification of  
747        optimal transplant conditions would greatly benefit from methodological advances that  
748        are both sensitive and facilitate reliable quantification of transplanted cell survival.  
749        Several new methods exist for quantifying transplant survival, including *in vivo* and *ex*  
750        *vivo* bioluminescence and fluorescence. Having established that HIF-1 $\alpha$  increased  
751        transplant survival using stereological quantification, we assessed the ability of *ex vivo*  
752        fluorescent imaging and *in vivo* bioluminescent imaging to detect the improvement in  
753        survival. Neither approach detected the improvement in transplant survival. Thus, for rat  
754        spinal cord transplants, histological quantification using non-biased stereology remains  
755        the most sensitive and reliable method for determining differences in transplant survival.

756

757        **Transplanted cells die within the first 2-3 days when transplanted into the sub-**  
758        **acutely injured spinal cord**

759        Several different cell types are currently in human testing for SCI repair  
760        (clinicaltrials.gov). Initial reports from human clinical trials indicate that cell transplants  
761        are safe (Tabakow et al., 2013; Shin et al., 2015; Anderson et al., 2017) but that the  
762        functional effects of cell transplants alone are limited. Ultimately, the effects of cell  
763        transplants will depend on both the cell type transplanted and the summation of the  
764        changes (both beneficial and potentially detrimental) that occur within the transplanted  
765        tissue. Because transplants persist long-term, an often-overlooked concern which may  
766        impact transplant and tissue function is the acute death of the majority of transplanted  
767        cells (Barakat et al., 2005; Hill et al., 2006; Karimi-Abdolrezaee et al., 2006; Hill et al.,  
768        2007).

769 To both maximize transplant efficacy and design superior anti-cell death  
770 interventions, establishing when this death occurs is needed. Here, using daily *in vivo*  
771 bioluminescence imaging and histological confirmation, we narrow the time window of  
772 transplanted cell death to the first 2 days post-TP (Fig. 1). The current reduction in  
773 bioluminescence following SC transplantation parallels both the decrease in  
774 transplanted cell number (Barakat et al., 2005; Hill et al., 2007; Pearse et al., 2007) and  
775 bioluminescence determined in previous rodent spinal cord transplant experiments  
776 (Okada et al., 2005; Kumagai et al., 2009; Takahashi et al., 2011; Ozdemir et al., 2012;  
777 Roet et al., 2012; Nishimura et al., 2013; Iwai et al., 2014). Although our  
778 bioluminescence results are similar to previous reports, previous studies generally  
779 report a slightly more prolonged decrease in bioluminescence, where light levels  
780 plateau by 4 dpi (Okada et al., 2005; Ozdemir et al., 2012), 7 dpi (Nishimura et al.,  
781 2013) or 15 dpi (Roet et al., 2012) compared to the 2 days observed here. Our results  
782 with SC grafts in sub-acute rat contusion SCIs most resemble those of neural stem  
783 cell/progenitor cell grafts in sub-acute mouse contusion SCIs, where bioluminescent  
784 activity decreases by ~80% and plateaus by 4 days post-TP, the earliest time point  
785 presented (Okada et al., 2005; Nishimura et al., 2013). Differences in injury model, cell  
786 type, transplant location, mechanism of luciferase expression, and time of  
787 transplantation between the studies likely contribute to the variability in the results  
788 reported between this and previous studies. Collectively, this and previous studies  
789 assessing transplant survival/death establish that transplant death occurs in all cell  
790 transplants, and that the death occurs in a narrow, acute window immediately post-TP.

791 The largest contributor to transplant death is likely the transplant environment (Hill et  
792 al., 2006; Nishimura et al., 2013; Piltti et al., 2013). SCI results in complex biochemical

793 and cellular changes that could contribute to the death of the transplanted cells,  
794 including: hypoxia, ischemia, oxidative and nitrosative stress, inflammation and immune  
795 mediators, decreased growth factors, and an altered extra-cellular matrix (Ahuja et al.,  
796 2017). This has led to the use of a multimodal transplant paradigm that includes a  
797 substrate, multiple growth factors, and a pharmacological inhibitor of cell death along  
798 with the cells (Lu et al., 2012; Robinson and Lu, 2017). Although effective, clinical  
799 translation of this approach will be difficult. The acute window of death determined here  
800 indicates that if interventions that protect the cells acutely can be identified, long-term  
801 inclusion of multiple factors is unlikely to be required.

802

### 803 **HIF-1 $\alpha$ protects SCs from oxidative stress and enhances transplant survival**

804 HIF-1 $\alpha$  is a key regulator of cellular adaptations to stress, including hypoxic, ischemic  
805 and oxidative stress. In the injured brain, elevating HIF-1 $\alpha$  either by hypoxic  
806 preconditioning or overexpression is sufficient to reduce transplant death (Theus et al.,  
807 2008) and enhance transplanted survival (Wu et al., 2010; Wakai et al., 2016).  
808 Recently, hypoxic preconditioning was shown to protect BMSC transplants in the injured  
809 spinal cord (Wang et al., 2018). HIF-1 $\alpha$  regulates the transcription of more than 100  
810 targets, including key mediators of angiogenesis and tissue vascularization (e.g., VEGF)  
811 (Forsythe et al., 1996; Ryan et al., 1998) and glycolysis and glucose metabolism (e.g.,  
812 enolase) (Semenza et al., 1994; Semenza et al., 1996). Here, we show that elevating  
813 HIF-1 $\alpha$  in SCs enhances nuclear levels of HIF-1 $\alpha$  in the cells and HIF transcriptional  
814 targets implicated in angiogenesis (VEGF; Fig 2) and glycolysis (enolase; Fig 2).

815 *In vitro*, HIF-1 $\alpha$ 's effects on cell survival depend on the mechanism of cell death  
816 induction (Fig 3A-D). This is similar to previous work in neurons (Halterman and

817 Federoff, 1999; Aminova et al., 2005). Although HIF-1 $\alpha$  is generally considered  
818 protective, among its transcription targets are pro-death genes linked to apoptosis and  
819 autophagy (Chen et al., 2009) and, under some circumstances, HIF-1 $\alpha$  augments cell  
820 death (Aminova et al., 2005; Vangeison et al., 2008). We observed that elevation of  
821 HIF-1 $\alpha$  protects SCs against oxidative stress (Fig 3A) and DNA damage (Fig 3B), is  
822 slightly detrimental upon activation of the unfolded protein response (UPS) (Fig 3D),  
823 and has no effect on ER stress (Fig 3C). With the exception of the response to oxidative  
824 stress, the magnitude and breadth of the survival changes in SCs in response to the  
825 inducers of cell death tested was limited. This is in contrast to neurons, where HIF-1 $\alpha$   
826 affords substantial protection against DNA damage, ER stress, and UPS activation, but  
827 is pro-death in response to glutamate-induced oxidative stress (Aminova et al., 2005). It  
828 is well-established that cellular sensitivity to cell death and HIF-1 $\alpha$ 's effects are cell type  
829 and context-dependent (Chen et al., 2009). Compared to neurons (Aminova et al.,  
830 2005), SCs were relatively resistant to DNA damage, ER Ca<sup>++</sup> release and induction of  
831 autophagy by initiation of the unfolded protein response. This could reflect a greater  
832 adaptability of SCs to harsh environments and/or the ability of SCs to modify their  
833 phenotype (e.g., SCs undergo substantial remodeling when they de-differentiate  
834 following peripheral nerve injury). This could account for the slightly higher survival rate  
835 of SCs (Barakat et al., 2005; Hill et al., 2007; Pearse et al., 2007) than neurons or  
836 neural progenitors (Barker et al., 1996; Karimi-Abdolrezaee et al., 2006) following  
837 transplantation. It is postulated that mild hypoxia leads to expression of adaptive HIF-  
838 1 $\alpha$  responses, whereas severe or prolonged exposure leads to the expression of pro-  
839 death genes (Halterman et al., 1999). The greater adaptability of SCs to harsh  
840 environments could also account for the differences between SCs and neurons exposed

841 to oxidative stress. The specific cell death inducers that impact transplant survival  
842 remain to be established. Further studies to identify and test the mediators of  
843 transplanted cell survival/death are necessary to establish the context under which HIF-  
844  $1\alpha$  and other pro-survival interventions affect transplant survival in a cell and  
845 environment-specific manner.

846 Elevation of HIF- $1\alpha$  in SCs protects SCs against oxidative damage (Fig 3A), to which  
847 SCs have been shown to be sensitive (Hill et al., 2010). In response to  $H_2O_2$  treatment,  
848 HIF- $1\alpha$  protected SCs to a similar level as inhibition of calpain-mediated cell death (Hill  
849 et al., 2010). In the vestibular system, SCs elevate HIF in response to oxidative stress,  
850 but it is not sufficient to prevent death (Riva et al., 2007), suggesting that the  
851 endogenous adaptive response of SCs to oxidative stress is insufficient to counteract  
852 the oxidative damage. Similarly, examination of the levels of HIF- $1\alpha$  in the spinal cord  
853 following transplantation indicate that SCs fail to initiate the HIF- $1\alpha$  adaptive response  
854 within the first 8 h after transplantation (unpublished data). Blocking lipid peroxidation, a  
855 consequence of oxidative damage, *in vitro* protects SCs but is insufficient to protect a  
856 variety of transplanted cells (Karlsson et al., 2002), including SCs (Hill et al., 2010). It is  
857 possible that counteracting oxidative stress is the wrong target for transplant protection.  
858 Alternatively, current treatments may not effectively reduce the generation of reactive  
859 oxygen species and subsequent oxidative stress. As HIF- $1\alpha$  is a regulator of diverse  
860 biological pathways, including oxygen supply and utilization (Dengler et al., 2014), it  
861 may afford better protection against oxidative damage than previous approaches.  
862 Moreover, HIF not only activates transcriptional programs that lead to decreased ROS  
863 production (Semenza, 2011), but, in response to hypoxia, generation of ROS is  
864 necessary to increase HIF- $1\alpha$ , making it a sensor of ROS (Chandel et al., 2000). The

865 mechanism by which HIF is stabilized in response to ROS is not yet known, however,  
866 ROS are postulated to increase HIF-1 $\alpha$  levels by interfering with HIF's hydroxylation by  
867 the HIF-prolyl hydroxylases at Pro<sup>402</sup> and Pro<sup>564</sup> and Factor Inhibiting HIF (FIH) at  
868 asparagine (Asn<sup>803</sup>) (Semenza, 2011). This implies that oxidative stress could augment  
869 HIF-1 $\alpha$  stability and activity, further increasing its cellular functions. In the current study,  
870 the HIF construct used contains aa 1-529 of HIF. Thus, one of the hydroxylation sites,  
871 Pro<sup>402</sup>, is retained. It is therefore possible that the enhanced protective effects in  
872 response to oxidative stress arise from greater elevation in the levels of HIF in this  
873 condition.

874 HIF-1 $\alpha$  increases the survival of SCs transplanted into the sub-acutely injured spinal  
875 cord (Fig 4 A-G). This result is similar to previous studies in which direct or indirect  
876 elevation of HIF-1 $\alpha$  enhances transplant survival of cells transplanted into the damaged  
877 brain (Theus et al., 2008; Wu et al., 2010; Wakai et al., 2016), heart (Zhang et al.,  
878 2001), and pancreas (Stokes et al., 2013). Although expression of HIF-1 $\alpha$  protected the  
879 cells, the increase in transplant survival with HIF-1 $\alpha$  was smaller than in previous spinal  
880 cord transplant studies targeting trophic support, anoikis, and/or cell death signaling  
881 (Golden et al., 2007; Hill et al., 2010; Patel et al., 2010; Lu et al., 2012; Robinson and  
882 Lu, 2017; Cerqueira et al., 2018). It is well-established that prolonged overexpression of  
883 HIF in transplanted cells induces tumor formation (Kung et al., 2000). We chose to use  
884 low constitutive HIF expression to mitigate this potential problem. A greater increase in  
885 HIF-1 $\alpha$  transcription may be required over the low-level HIF-1 $\alpha$  induction of this study.  
886 Higher levels of HIF transcription are achievable with higher viral MOIs and  
887 pharmacological stabilization of HIF (unpublished preliminary studies). Alternatively,

888 activation of other transcription factors that mediate other key cellular programs (e.g.,  
889 Nrf2 and NF $\kappa$ B) may provide greater survival benefits than HIF-1 $\alpha$ .

890 Elevation of HIF-1 $\alpha$  can result in the doubling of transplant size (Wu et al., 2010;  
891 Wakai et al., 2016). This is substantially greater than the enhancement in survival  
892 achieved in the current study. Several factors could contribute to this difference in  
893 transplant survival including differences in the levels of HIF-1 $\alpha$  in the cells post-TP. One  
894 limitation of this and previous studies is that although HIF-1 $\alpha$  levels were measured in  
895 the cells prior to TP, they have not been measured post-TP. Cell type differences could  
896 also affect both the sensitivity of the cells to the transplant environment and the  
897 specifics of the transcriptional program(s) activated (Chi et al., 2006; Benita et al., 2009;  
898 Lendahl et al., 2009). Previous studies have examined stem cells or BMSCs, cell types  
899 that reside in low-oxygen niches. It is currently unclear how oxygen tension impacts  
900 adult de-differentiated SCs and which specific transcriptional programs are activated in  
901 SCs in response to elevation of HIF-1 $\alpha$ .

902 This study establishes that increasing HIF-1 $\alpha$  is cytoprotective for transplanted SCs.  
903 It also demonstrates the feasibility of targeting HIF (and other transcription factors) as  
904 an approach to enhance transplanted cell survival. It supports the hypothesis that  
905 activating adaptive responses in transplanted cells can protect them following  
906 transplantation. This paves the way to test pharmacological interventions that  
907 temporarily elevate HIF (or other transcription factors) prior to transplantation in order to  
908 test whether overcoming the initial 2-day window in which the cells die is sufficient.  
909 Ongoing studies in the lab are testing the efficacy of clinically-feasible paradigms to  
910 elevate HIF-1 $\alpha$  transiently and substantially.

911



912 **Development of additional, rapid, reliable methods to quantify transplant survival**  
913 **is needed**

914 Stereology proved to be the most sensitive method for detecting differences in  
915 transplant survival. In the injured spinal cord, IVIS imaging is able to detect a decrease  
916 in transplanted cells over time [Fig 1A; (Okada et al., 2005; Takahashi et al., 2011; Roet  
917 et al., 2012; Nishimura et al., 2013)]. In cancer studies, it detects increases in tumor  
918 cells (Rehemtulla et al., 2000). Under the current conditions, neither *in vivo*  
919 bioluminescence imaging (Fig 4 J-K) nor *ex vivo* fluorescence imaging of spinal cords  
920 (Fig 4 H-I) was sensitive enough to detect the 35% improvement in transplant survival  
921 verified by stereology. Based on post-hoc power analyses, a large number of animals  
922 would be required to detect a difference with either of these methods ( $\geq 14$ ). This  
923 decreases the utility of both *in vivo* bioluminescent imaging and *ex vivo* fluorescent  
924 imaging as primary screens for transplant survival in the injured rat spinal cord. In  
925 theory, bioluminescent and fluorescent imaging can detect as few as 1000 cells  
926 (Terrovitis et al., 2010); in practice, several factors limit light production/detection. For  
927 spinal cord transplants, the location of the spinal cord deep within the vertebral column  
928 is particularly problematic due to tissue light absorption. Use of longer light wavelengths  
929 (i.e., far-red/near-infrared wavelengths) may circumvent this problem. Following SCI,  
930 several conditions within the transplant/injury site impact d-luciferin availability (e.g.,  
931 altered vasculature) or enzymatic activity (e.g., reduced levels of required luciferin co-  
932 factors, ATP and O<sub>2</sub>), which substantially impact light production and contribute to the  
933 variability in light detected between and within cases. This makes it difficult to ascertain  
934 whether different light levels detected arise from variability in the number of cells initially  
935 transplanted, delivery of d-luciferin to the cells, or differences in survival. Fluorescence-



936 based probes overcome the limitations associated with d-luciferin administration. Far-  
937 red/near infrared constructs for IVIS imaging have been developed (Shcherbo et al.,  
938 2007; Rumyantsev et al., 2016). They may facilitate *in vivo* imaging of cells following  
939 transplantation. One concern, however, is our failure to detect differences in transplant  
940 survival with *ex vivo* fluorescent imaging of GFP transplants where penetration of light  
941 through the tissue (i.e., bone, muscle, skin) is not required. This suggests additional  
942 technological advances are required for the use of fluorescence-based assays of  
943 transplant survival in whole tissues or animals. Current methods to quantify the number  
944 of surviving cells are either time-consuming (e.g., stereology), or require pulverization of  
945 the tissue (western blotting, qPCR) which prevents further examination, or either have  
946 too much variability or are not sensitive enough to detect anything but robust changes in  
947 survival (*in vivo* bioluminescent imaging and *ex vivo* fluorescent imaging). Additional  
948 rapid, sensitive approaches for screening transplant survival are needed to facilitate  
949 identification of prosurvival strategies. Until better assessments are developed,  
950 stereological quantification remains the most reliable method.

951

## 952 **Summary and conclusions**

953 To advance the field, and to maximize the therapeutic use and benefits of cellular  
954 transplants for human clinical use, there is a critical need to develop strategies that  
955 effectively promote and permit rapid assessment of transplant survival. We have  
956 identified the narrow time window in which transplanted cells die within the injured  
957 spinal cord, thus establishing the time window in which cytoprotection should be  
958 targeted to counteract transplanted cell death. We tested the effects of elevating HIF-1 $\alpha$   
959 in cells, and identify HIF-1 $\alpha$  as a transcription factor that protects transplanted cells.

960 Lastly, we tested three approaches to quantifying transplant survival, and demonstrate  
961 that stereology remains the most reliable until faster, more sensitive methods can be  
962 developed. We anticipate that interventions that specifically harness cellular adaptive  
963 responses prior to transplantation could obviate the need to add additional components  
964 to cells at the time of transplantation and thus aid in the adoption of this approach to  
965 current clinical transplant protocols.

966

967

968

969 **References:**

- 970 Afshari FT, Kwok JC, White L, Fawcett JW (2010) Schwann cell migration is integrin-  
 971 dependent and inhibited by astrocyte-produced aggrecan. *Glia* 58:857-869.
- 972 Ahuja CS, Wilson JR, Nori S, Kotter MRN, Druschel C, Curt A, Fehlings MG (2017)  
 973 Traumatic spinal cord injury. *Nat Rev Dis Primers* 3:17018.
- 974 Aminova LR, Siddiq A, Ratan RR (2008) Antioxidants, HIF prolyl hydroxylase inhibitors  
 975 or short interfering RNAs to BNIP3 or PUMA, can prevent prodeath effects of the  
 976 transcriptional activator, HIF-1alpha, in a mouse hippocampal neuronal line.  
 977 *Antioxid Redox Sign* 10:1989-1998.
- 978 Aminova LR, Chavez JC, Lee J, Ryu H, Kung A, LaManna JC, Ratan RR (2005)  
 979 Prosurvival and prodeath effects of hypoxia-inducible factor-1alpha stabilization  
 980 in a murine hippocampal cell line. *J Biol Chem* 280:3996-4003.
- 981 Anderson KD, Guest JD, Dietrich WD, Bartlett Bunge M, Curiel R, Dididze M, Green BA,  
 982 Khan A, Pearse DD, Saraf-Lavi E, Widerstrom-Noga E, Wood P, Levi AD (2017)  
 983 Safety of Autologous Human Schwann Cell Transplantation in Subacute Thoracic  
 984 Spinal Cord Injury. *J Neurotraum* 34:2950-2963.
- 985 Araos J, Sleeman JP, Garvalov BK (2018) The role of hypoxic signalling in metastasis:  
 986 towards translating knowledge of basic biology into novel anti-tumour strategies.  
 987 *Clin Exp Metastas* 35:563-599.
- 988 Bakshi A, Keck CA, Koshkin VS, LeBold DG, Siman R, Snyder EY, McIntosh TK (2005)  
 989 Caspase-mediated cell death predominates following engraftment of neural  
 990 progenitor cells into traumatically injured rat brain. *Brain Research* 1065:8-19.
- 991 Barakat DJ, Gaglani SM, Neravetla SR, Sanchez AR, Andrade CM, Pressman Y, Puzis  
 992 R, Garg MS, Bunge MB, Pearse DD (2005) Survival, integration, and axon  
 993 growth support of glia transplanted into the chronically contused spinal cord. *Cell*  
 994 *Transplant* 14:225-240.
- 995 Barker RA, Dunnett SB, Faissner A, Fawcett JW (1996) The time course of loss of  
 996 dopaminergic neurons and the gliotic reaction surrounding grafts of embryonic  
 997 mesencephalon to the striatum. *Exp Neurol* 141:79-93.
- 998 Barriga EH, Maxwell PH, Reyes AE, Mayor R (2013) The hypoxia factor Hif-1alpha  
 999 controls neural crest chemotaxis and epithelial to mesenchymal transition. *J Cell*  
 1000 *Biol* 201:759-776.
- 1001 Benita Y, Kikuchi H, Smith AD, Zhang MQ, Chung DC, Xavier RJ (2009) An integrative  
 1002 genomics approach identifies Hypoxia Inducible Factor-1 (HIF-1)-target genes  
 1003 that form the core response to hypoxia. *Nucleic Acids Res* 37:4587-4602.
- 1004 Cerqueira SR, Lee YS, Cornelison RC, Mertz MW, Wachs RA, Schmidt CE, Bunge MB  
 1005 (2018) Decellularized peripheral nerve supports Schwann cell transplants and  
 1006 axon growth following spinal cord injury. *Biomaterials* 177:176-185.
- 1007 Chandel NS, McClintock DS, Feliciano CE, Wood TM, Melendez JA, Rodriguez AM,  
 1008 Schumacker PT (2000) Reactive oxygen species generated at mitochondrial  
 1009 complex III stabilize hypoxia-inducible factor-1alpha during hypoxia: a  
 1010 mechanism of O2 sensing. *J Biol Chem* 275:25130-25138.
- 1011 Chen W, Ostrowski RP, Obenaus A, Zhang JH (2009) Prodeath or prosurvival: two  
 1012 facets of hypoxia inducible factor-1 in perinatal brain injury. *Exp Neurol* 216:7-15.
- 1013 Chen X, Zhang X, Larson CS, Baker MS, Kaufman DB (2006) In vivo bioluminescence  
 1014 imaging of transplanted islets and early detection of graft rejection.  
 1015 *Transplantation* 81:1421-1427.

- 1016 Chi JT, Wang Z, Nuyten DS, Rodriguez EH, Schaner ME, Salim A, Wang Y, Kristensen  
1017 GB, Helland A, Borresen-Dale AL, Giaccia A, Longaker MT, Hastie T, Yang GP,  
1018 van de Vijver MJ, Brown PO (2006) Gene expression programs in response to  
1019 hypoxia: cell type specificity and prognostic significance in human cancers. *PLoS*  
1020 *Med* 3:e47.
- 1021 Chu K, Jung KH, Kim SJ, Lee ST, Kim J, Park HK, Song EC, Kim SU, Kim M, Lee SK,  
1022 Roh JK (2008) Transplantation of human neural stem cells protect against  
1023 ischemia in a preventive mode via hypoxia-inducible factor-1alpha stabilization in  
1024 the host brain. *Brain Res* 1207:182-92.
- 1025 Dengler VL, Galbraith M, Espinosa JM (2014) Transcriptional regulation by hypoxia  
1026 inducible factors. *Crit Rev Biochem Mol* 49:1-15.
- 1027 Ding WX, Ni HM, Gao W, Hou YF, Melan MA, Chen X, Stolz DB, Shao ZM, Yin XM  
1028 (2007) Differential effects of endoplasmic reticulum stress-induced autophagy on  
1029 cell survival. *J Biol Chem* 282:4702-4710.
- 1030 Emgard M, Hallin U, Karlsson J, Bahr BA, Brundin P, Blomgren K (2003) Both apoptosis  
1031 and necrosis occur early after intracerebral grafting of ventral mesencephalic  
1032 tissue: a role for protease activation. *J Neurochem* 86:1223-1232.
- 1033 Forsythe JA, Jiang BH, Iyer NV, Agani F, Leung SW, Koos RD, Semenza GL (1996)  
1034 Activation of vascular endothelial growth factor gene transcription by hypoxia-  
1035 inducible factor 1. *Mol Cell Biol* 16:4604-4613.
- 1036 Golden KL, Pearse DD, Blits B, Garg MS, Oudega M, Wood PM, Bunge MB (2007)  
1037 Transduced Schwann cells promote axon growth and myelination after spinal  
1038 cord injury. *Exp Neurol* 207:203-217.
- 1039 Gomez-Sanchez JA et al. (2015) Schwann cell autophagy, myelinophagy, initiates  
1040 myelin clearance from injured nerves. *J Cell Biol* 210:153-168.
- 1041 Halterman MW, Federoff HJ (1999) HIF-1alpha and p53 promote hypoxia-induced  
1042 delayed neuronal death in models of CNS ischemia. *Exp Neurol* 159:65-72.
- 1043 Halterman MW, Miller CC, Federoff HJ (1999) Hypoxia-inducible factor-1alpha mediates  
1044 hypoxia-induced delayed neuronal death that involves p53. *J Neurosci* 19:6818-  
1045 6824.
- 1046 Hill CE, Moon LD, Wood PM, Bunge MB (2006) Labeled Schwann cell transplantation:  
1047 cell loss, host Schwann cell replacement, and strategies to enhance survival.  
1048 *Glia* 53:338-343.
- 1049 Hill CE, Guller Y, Raffa SJ, Hurtado A, Bunge MB (2010) A calpain inhibitor enhances  
1050 the survival of schwann cells in vitro and after transplantation into the injured  
1051 spinal cord. *J Neurotraum* 27:1685-1695.
- 1052 Hill CE, Hurtado A, Blits B, Bahr BA, Wood PM, Bartlett BM, Oudega M (2007) Early  
1053 necrosis and apoptosis of Schwann cells transplanted into the injured rat spinal  
1054 cord. *Eur J Neurosci* 26:1433-1445.
- 1055 Iwai H, Nori S, Nishimura S, Yasuda A, Takano M, Tsuji O, Fujiyoshi K, Toyama Y,  
1056 Okano H, Nakamura M (2014) Transplantation of neural stem/progenitor cells at  
1057 different locations in mice with spinal cord injury. *Cell Transplant* 23:1451-1464.
- 1058 Karimi-Abdolrezaee S, Eftekharpour E, Wang J, Morshead CM, Fehlings MG (2006)  
1059 Delayed transplantation of adult neural precursor cells promotes remyelination  
1060 and functional neurological recovery after spinal cord injury. *J Neurosci* 26:3377-  
1061 3389.

- 1062 Karlsson J, Emgard M, Brundin P (2002) Comparison between survival of lazaroïd-  
 1063 treated embryonic nigral neurons in cell suspensions, cultures and transplants.  
 1064 *Brain Res* 955:268-280.
- 1065 Kim DE, Tsuji K, Kim YR, Mueller FJ, Eom HS, Snyder EY, Lo EH, Weissleder R,  
 1066 Schellingerhout D (2006) Neural stem cell transplant survival in brains of mice:  
 1067 assessing the effect of immunity and ischemia by using real-time bioluminescent  
 1068 imaging. *Radiology* 241:822-830.
- 1069 Kumagai G, Okada Y, Yamane J, Nagoshi N, Kitamura K, Mukaino M, Tsuji O, Fujiyoshi  
 1070 K, Katoh H, Okada S, Shibata S, Matsuzaki Y, Toh S, Toyama Y, Nakamura M,  
 1071 Okano H (2009) Roles of ES cell-derived gliogenic neural stem/progenitor cells in  
 1072 functional recovery after spinal cord injury. *PLoS One* 4:e7706.
- 1073 Kung AL, Wang S, Klco JM, Kaelin WG, Livingston DM (2000) Suppression of tumor  
 1074 growth through disruption of hypoxia-inducible transcription. *Nat Med* 6:1335-  
 1075 1340.
- 1076 Lendahl U, Lee KL, Yang H, Poellinger L (2009) Generating specificity and diversity in  
 1077 the transcriptional response to hypoxia. *Nat Rev Genet* 10:821-832.
- 1078 Li HS, Zhou YN, Li L, Li SF, Long D, Chen XL, Zhang JB, Feng L, Li YP (2019) HIF-  
 1079 1 $\alpha$  protects against oxidative stress by directly targeting mitochondria. *Redox*  
 1080 *Biol*:101109.
- 1081 Lu P, Wang Y, Graham L, McHale K, Gao M, Wu D, Brock J, Blesch A, Rosenzweig ES,  
 1082 Havton LA, Zheng B, Conner JM, Marsala M, Tuszynski MH (2012) Long-  
 1083 distance growth and connectivity of neural stem cells after severe spinal cord  
 1084 injury. *Cell* 150:1264-1273.
- 1085 McDonald JW, Liu XZ, Qu Y, Liu S, Mickey SK, Turetsky D, Gottlieb DI, Choi DW  
 1086 (1999) Transplanted embryonic stem cells survive, differentiate and promote  
 1087 recovery in injured rat spinal cord [see comments]. *Nat Med* 5:1410-1412.
- 1088 Morrissey TK, Kleitman N, Bunge RP (1991) Isolation and functional characterization of  
 1089 Schwann cells derived from adult peripheral nerve. *J Neurosci* 11:2433-2442.
- 1090 Mundt-Petersen U, Petersen A, Emgard M, Dunnett SB, Brundin P (2000) Caspase  
 1091 inhibition increases embryonic striatal graft survival. *Exp Neurol* 164:112-120.
- 1092 Murry CE, Jennings RB, Reimer KA (1986) Preconditioning with ischemia: a delay of  
 1093 lethal cell injury in ischemic myocardium. *Circulation* 74:1124-1136.
- 1094 Nakao N, Frodl EM, Duan WM, Widner H, Brundin P (1994) Lazaroids improve the  
 1095 survival of grafted rat embryonic dopamine neurons. *P Natl Acad Sci USA*  
 1096 91:12408-12412.
- 1097 Ney PA (2015) Mitochondrial autophagy: Origins, significance, and role of BNIP3 and  
 1098 NIX. *Biochim Biophys Acta* 1853:2775-2783.
- 1099 Nishimura S, Yasuda A, Iwai H, Takano M, Kobayashi Y, Nori S, Tsuji O, Fujiyoshi K,  
 1100 Ebise H, Toyama Y, Okano H, Nakamura M (2013) Time-dependent changes in  
 1101 the microenvironment of injured spinal cord affects the therapeutic potential of  
 1102 neural stem cell transplantation for spinal cord injury. *Mol Brain* 6:3.
- 1103 Okada S, Ishii K, Yamane J, Iwanami A, Ikegami T, Katoh H, Iwamoto Y, Nakamura M,  
 1104 Miyoshi H, Okano HJ, Contag CH, Toyama Y, Okano H (2005) In vivo imaging of  
 1105 engrafted neural stem cells: its application in evaluating the optimal timing of  
 1106 transplantation for spinal cord injury. *FASEB J* 19:1839-1841.
- 1107 Ozdemir M, Attar A, Kuzu I, Ayten M, Ozgencil E, Bozkurt M, Dalva K, Uckan D, Kilic E,  
 1108 Sancak T, Kanpolat Y, Beksac M (2012) Stem cell therapy in spinal cord injury: in



- 1109 vivo and postmortem tracking of bone marrow mononuclear or mesenchymal  
 1110 stem cells. *Stem Cell Rev* 8:953-962.
- 1111 Patel V, Joseph G, Patel A, Patel S, Bustin D, Mawson D, Tuesta LM, Puentes R,  
 1112 Ghosh M, Pearse DD (2010) Suspension matrices for improved Schwann-cell  
 1113 survival after implantation into the injured rat spinal cord. *J Neurotraum* 27:789-  
 1114 801.
- 1115 Pearse DD, Sanchez AR, Pereira FC, Andrade CM, Puzis R, Pressman Y, Golden K,  
 1116 Kitay BM, Blits B, Wood PM, Bunge MB (2007) Transplantation of Schwann cells  
 1117 and/or olfactory ensheathing glia into the contused spinal cord: Survival,  
 1118 migration, axon association, and functional recovery. *Glia* 55:976-1000.
- 1119 Piltti KM, Salazar DL, Uchida N, Cummings BJ, Anderson AJ (2013) Safety of epicenter  
 1120 versus intact parenchyma as a transplantation site for human neural stem cells  
 1121 for spinal cord injury therapy. *Stem Cell Transl Med* 2:204-216.
- 1122 Pugh CW (2016) Modulation of the Hypoxic Response. *Adv Exp Med Biol* 903:259-271.
- 1123 Ratan RR et al. (2008) Small molecule activation of adaptive gene expression: tilorone  
 1124 or its analogs are novel potent activators of hypoxia inducible factor-1 that  
 1125 provide prophylaxis against stroke and spinal cord injury. *Ann NY Acad Sci*  
 1126 1147:383-94.
- 1127 Rehemtulla A, Stegman LD, Cardozo SJ, Gupta S, Hall DE, Contag CH, Ross BD  
 1128 (2000) Rapid and quantitative assessment of cancer treatment response using in  
 1129 vivo bioluminescence imaging. *Neoplasia* 2:491-495.
- 1130 Riva C, Donadieu E, Magnan J, Lavieille JP (2007) Age-related hearing loss in CD/1  
 1131 mice is associated to ROS formation and HIF target proteins up-regulation in the  
 1132 cochlea. *Exp Gerontol* 42:327-336.
- 1133 Robinson J, Lu P (2017) Optimization of trophic support for neural stem cell grafts in  
 1134 sites of spinal cord injury. *Exp Neurol* 291:87-97.
- 1135 Roet KC, Eggers R, Verhaagen J (2012) Noninvasive bioluminescence imaging of  
 1136 olfactory ensheathing glia and schwann cells following transplantation into the  
 1137 lesioned rat spinal cord. *Cell Transplant* 21:1853-1865.
- 1138 Rumyantsev KA, Turoverov KK, Verkhusha VV (2016) Near-infrared bioluminescent  
 1139 proteins for two-color multimodal imaging. *Sci Rep-UK* 6:36588.
- 1140 Ruthenborg RJ, Ban JJ, Wazir A, Takeda N, Kim JW (2014) Regulation of wound  
 1141 healing and fibrosis by hypoxia and hypoxia-inducible factor-1. *Mol Cells* 37:637-  
 1142 643.
- 1143 Ryan HE, Lo J, Johnson RS (1998) HIF-1 alpha is required for solid tumor formation  
 1144 and embryonic vascularization. *EMBO J* 17:3005-3015.
- 1145 Schodel J, Mole DR, Ratcliffe PJ (2013) Pan-genomic binding of hypoxia-inducible  
 1146 transcription factors. *Biol Chem* 394:507-517.
- 1147 Semenza GL (2007) Hypoxia-inducible factor 1 (HIF-1) pathway. *Sci STKE* 2007:cm8.
- 1148 Semenza GL (2011) Hypoxia-inducible factor 1: regulator of mitochondrial metabolism  
 1149 and mediator of ischemic preconditioning. *Biochim Biophys Acta* 1813:1263-  
 1150 1268.
- 1151 Semenza GL (2012) Hypoxia-inducible factors in physiology and medicine. *Cell*  
 1152 148:399-408.
- 1153 Semenza GL, Roth PH, Fang HM, Wang GL (1994) Transcriptional regulation of genes  
 1154 encoding glycolytic enzymes by hypoxia-inducible factor 1. *J Biol Chem*  
 1155 269:23757-23763.

- 1156 Semenza GL, Jiang BH, Leung SW, Passantino R, Concordet JP, Maire P, Giallongo A  
1157 (1996) Hypoxia response elements in the aldolase A, enolase 1, and lactate  
1158 dehydrogenase A gene promoters contain essential binding sites for hypoxia-  
1159 inducible factor 1. *J Biol Chem* 271:32529-32537.
- 1160 Shcherbo D, Merzlyak EM, Chepurnykh TV, Fradkov AF, Ermakova GV, Solovieva EA,  
1161 Lukyanov KA, Bogdanova EA, Zaisky AG, Lukyanov S, Chudakov DM (2007)  
1162 Bright far-red fluorescent protein for whole-body imaging. *Nat Methods* 4:741-  
1163 746.
- 1164 Shin JC, Kim KN, Yoo J, Kim IS, Yun S, Lee H, Jung K, Hwang K, Kim M, Lee IS, Shin  
1165 JE, Park KI (2015) Clinical Trial of Human Fetal Brain-Derived Neural  
1166 Stem/Progenitor Cell Transplantation in Patients with Traumatic Cervical Spinal  
1167 Cord Injury. *Neural Plast* 2015:630932.
- 1168 Smirnova NA, Rakhman I, Moroz N, Basso M, Payappilly J, Kazakov S, Hernandez-  
1169 Guzman F, Gaisina IN, Kozikowski AP, Ratan RR, Gazaryan IG (2010) Utilization  
1170 of an in vivo reporter for high throughput identification of branched small  
1171 molecule regulators of hypoxic adaptation. *Chem Biol* 17:380-391.
- 1172 Stokes RA, Cheng K, Deters N, Lau SM, Hawthorne WJ, O'Connell PJ, Stolp J, Grey S,  
1173 Loudovaris T, Kay TW, Thomas HE, Gonzalez FJ, Gunton JE (2013) Hypoxia-  
1174 inducible factor-1alpha (HIF-1alpha) potentiates beta-cell survival after islet  
1175 transplantation of human and mouse islets. *Cell Transplant* 22:253-266.
- 1176 Tabakow P, Jarmundowicz W, Czapiga B, Fortuna W, Miedzybrodzki R, Czyz M, Huber  
1177 J, Szarek D, Okurowski S, Szewczyk P, Gorski A, Raisman G (2013)  
1178 Transplantation of autologous olfactory ensheathing cells in complete human  
1179 spinal cord injury. *Cell Transplant* 22:1591-1612.
- 1180 Takahashi Y, Tsuji O, Kumagai G, Hara CM, Okano HJ, Miyawaki A, Toyama Y, Okano  
1181 H, Nakamura M (2011) Comparative study of methods for administering neural  
1182 stem/progenitor cells to treat spinal cord injury in mice. *Cell Transplant* 20:727-  
1183 739.
- 1184 Terrovitis JV, Smith RR, Marban E (2010) Assessment and optimization of cell  
1185 engraftment after transplantation into the heart. *Circ Res* 106:479-494.
- 1186 Tetzlaff W, Okon EB, Karimi-Abdolrezaee S, Hill CE, Sparling JS, Plemel JR, Plunet  
1187 WT, Tsai EC, Baptiste D, Smithson LJ, Kawaja MD, Fehlings MG, Kwon BK  
1188 (2010) A Systematic Review of Cellular Transplantation Therapies for Spinal  
1189 Cord Injury. *J Neurotraum* 28:1611-1682.
- 1190 Theus MH, Wei L, Cui L, Francis K, Hu X, Keogh C, Yu SP (2008) In vitro hypoxic  
1191 preconditioning of embryonic stem cells as a strategy of promoting cell survival  
1192 and functional benefits after transplantation into the ischemic rat brain. *Exp*  
1193 *Neurol* 210:656-670.
- 1194 Thomas LW, Ashcroft M (2019) Exploring the molecular interface between hypoxia-  
1195 inducible factor signalling and mitochondria. *Cell Mol Life Sci* 76:1759-1777.
- 1196 Vangeison G, Carr D, Federoff HJ, Rempe DA (2008) The good, the bad, and the cell  
1197 type-specific roles of hypoxia inducible factor-1 alpha in neurons and astrocytes.  
1198 *J Neurosci* 28:1988-1993.
- 1199 Wakai T, Narasimhan P, Sakata H, Wang E, Yoshioka H, Kinouchi H, Chan PH (2016)  
1200 Hypoxic preconditioning enhances neural stem cell transplantation therapy after  
1201 intracerebral hemorrhage in mice. *J Cerebr Blood F Met* 36:2134-2145.

- 1202 Wang W, Huang X, Lin W, Qiu Y, He Y, Yu J, Xi Y, Ye X (2018) Hypoxic preconditioned  
1203 bone mesenchymal stem cells ameliorate spinal cord injury in rats via improved  
1204 survival and migration. *Int J Mol Med* 42:2538-2550.
- 1205 Wu W, Chen X, Hu C, Li J, Yu Z, Cai W (2010) Transplantation of neural stem cells  
1206 expressing hypoxia-inducible factor-1alpha (HIF-1alpha) improves behavioral  
1207 recovery in a rat stroke model. *J Clin Neurosci* 17:92-95.
- 1208 Yang C, Jiang L, Zhang H, Shimoda LA, DeBerardinis RJ, Semenza GL (2014) Analysis  
1209 of hypoxia-induced metabolic reprogramming. *Methods Enzymol* 542:425-455.
- 1210 Yu SP, Wei Z, Wei L (2013) Preconditioning strategy in stem cell transplantation  
1211 therapy. *Transl Stroke Res* 4:76-88.
- 1212 Zhang M, Methot D, Poppa V, Fujio Y, Walsh K, Murry CE (2001) Cardiomyocyte  
1213 grafting for cardiac repair: graft cell death and anti-death strategies. *J Mol Cell*  
1214 *Cardiol* 33:907-921.
- 1215

1216

1217

1218

1219

1220

1221

1222

1223

1224

1225

1226

1227

1228

1229

1230

1231 **Figure Legends:**

1232



1233 **Figure 1: Decrease in transplanted cells occurs within 2 days post-transplant,**  
1234 **after which time there is no further decrease in cell number.**  $2 \times 10^6$  GFP-luc SCs  
1235 were transplanted into the injured spinal cord 7 days post-injury. Transplanted cell  
1236 survival was assessed in live rats by *in vivo* bioluminescent imaging (A). The amount of  
1237 light produced by luciferase activity was quantified daily in the IVIS following d-luciferin  
1238 administration for up to 7 days (days 1-3, n=8-9; days 4-7, n=3-5). Following tissue  
1239 collection, the number of surviving GFP<sup>+</sup> transplanted cells was quantified at 3 days  
1240 (n=3) or 7 days (n=4) post-TP in the fixed, sectioned spinal cords by stereology (B).  
1241 Mean  $\pm$  SEM. \*, p=0.004. Figure Contributions: Veena Kandaswamy and Kerri Scorpio  
1242 performed this experiment; Caitlin Hill analyzed the data.

1243  
1244 **Figure 2: HIF-1 $\alpha$  protein and HIF-1 $\alpha$  target genes are elevated in SCs following**  
1245 **retrovirus administration.** Expression of mRNA for VP16, HIF-1 $\alpha$  and  $\beta$ -actin in  
1246 transfected SCs was confirmed by PCR in VP16 and VP16-HIF SCs (A). Protein  
1247 expression of VP16, HIF-1 $\alpha$ , HIF-2 $\alpha$ , VEGF, enolase and protein loading controls (GFP  
1248 or  $\beta$ -actin) in transfected SCs was assessed by western blotting (B). Protein expression  
1249 was normalized to the loading control. Relative intensity of VP16 expression is shown in  
1250 (C) and the fold change in protein expression relative to control SCs is shown for HIF-  
1251 1 $\alpha$  (D) HIF-2 $\alpha$  (E) VEGF (F) and enolase (G). Values are as follows: VP16 (control: 0.0  
1252  $\pm$  0.0; VP16:  $0.40 \pm 0.01$ ; VP16-HIF:  $0.41 \pm 0.00$ ); HIF-1 $\alpha$  (control:  $1.0 \pm 0.04$ ; VP16:  
1253  $1.0 \pm 0.04$ ; VP16-HIF:  $5.9 \pm 0.01$ ); HIF-2 $\alpha$  (control:  $1.0 \pm 0.01$ ; VP16:  $1.0 \pm 0.01$ ; VP16-  
1254 HIF:  $1.0 \pm 0.02$ ); VEGF (control:  $1.0 \pm 0.01$ ; VP16:  $1.02 \pm 0.02$ ; VP16-HIF:  $2.2 \pm 0.01$ );  
1255 Enolase (control:  $1.0 \pm 0.01$ ; VP16:  $1.0 \pm 0.04$ ; VP16-HIF:  $1.7 \pm 0.00$ ). n=3/group. Mean  
1256  $\pm$  SEM. \*, p < 0.0001. Figure Contributions: Veena Kandaswamy generated the VP16-

1257 HIF cells; Veena Kandaswamy performed the PCRs; Ying Dai performed the western  
1258 blots; Ying Dai and Caitlin Hill analyzed the data.

1259

1260 **Figure 3: Elevation of HIF-1 $\alpha$  inhibits, enhances, or has no effect on SC survival**

1261 **in response to different cell death inducers.** SC cultures in 96-well plates were  
1262 treated with various doses of H<sub>2</sub>O<sub>2</sub> (A), camptothecin (B), thapsigargin (C), or  
1263 tunicamycin (D) and survival assessed at either 3 h (H<sub>2</sub>O<sub>2</sub>) or 24 h (other inducers) by  
1264 MTS assay to assess the effects of elevation of HIF in response to oxidative stress,  
1265 DNA damage, ER Ca<sup>++</sup> release, and the UPR, respectively. n=3 independent  
1266 experiments/condition. Mean  $\pm$  SEM. \*, A: 3.9  $\mu$ M, p = 0.03; 16.3  $\mu$ M, p = 0.006; 31.3  
1267  $\mu$ M, p < 0.0001; 62.5  $\mu$ M, p = 0.03; B: 3  $\mu$ M, p = 0.002; 12  $\mu$ M, p = 0.014; D: 1  $\mu$ M, p =  
1268 0.037. Figure Contributions: Caitlin Hill and Jessica Curtin performed the experiments;  
1269 Caitlin Hill analyzed the data.

1270

1271 **Figure 4: HIF increases the survival of transplanted cells. This is detectable**

1272 **histologically by stereological quantification, but not by *ex vivo* fluorescent**

1273 **imaging of spinal cords or *in vivo* bioluminescent imaging.** 2x10<sup>6</sup> GFP-luc SCs

1274 were transplanted into the injured spinal cord 7 days post-SCI [control (n=7), VP16

1275 (n=6), or VP16-HIF (n=8)]. Seven days post-TP, transplant survival was quantified by

1276 histology (A-G) and *ex vivo* fluorescent imaging of spinal cords for GFP (H, I). In a

1277 subset of the rats [control (n=3), VP16 (n=4), or VP16-HIF (n=4)], transplant survival

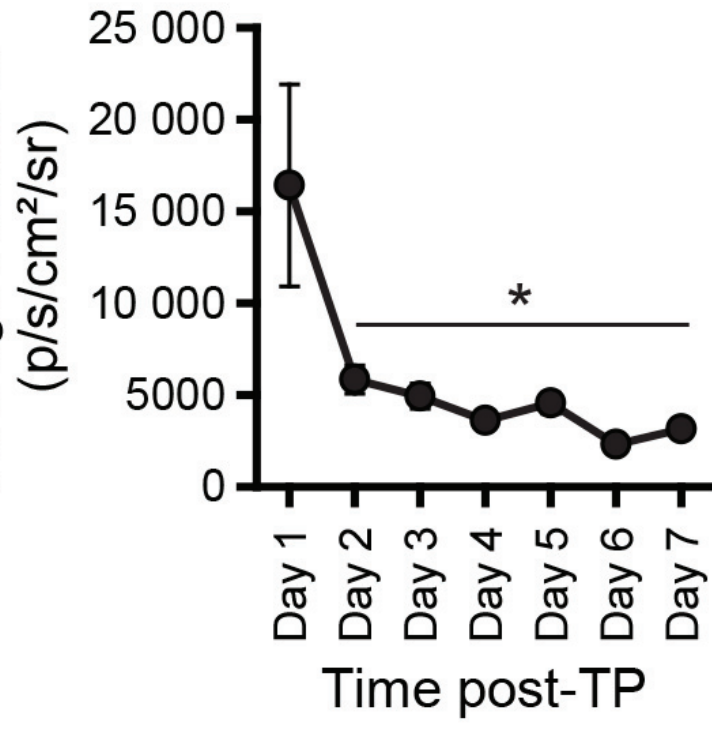
1278 was assessed by performing daily *in vivo* bioluminescent imaging on days 1-3 post-TP

1279 (J, K). Representative images of the transplants and the cells within the transplants 7

1280 days post-TP are shown for each group (A-F). More SCs survive when they express

1281 VP16-HIF, as determined by stereology (G). Results of quantification of the cell number  
 1282 by stereology (G). Images of representative spinal cord showing radiant efficiency of the  
 1283 *ex vivo* imaging for transplant GFP fluorescence 7 days post-TP (H). Quantification of  
 1284 radiant efficiency (I). Images of photon counts for bioluminescence activity of the  
 1285 transplanted cells for the first 3 days post-TP for each cell type transplanted (J) and  
 1286 quantification of light emitted (average radiance) (K). Mean  $\pm$  SEM. \*, G: control vs  
 1287 VP16-HIF,  $p = 0.0025$ ; VP16 vs VP16-HIF,  $p = 0.027$ ; K: d1 vs d2,  $p = 0.01$ ; d1 vs d3,  $p$   
 1288  $= 0.031$ . Figure Contributions: Caitlin Hill, Brian David, Jessica Curtin, and David  
 1289 Goldberg performed the experiment; Caitlin Hill and Brian David analyzed the data.

# A



# B

